

BEST AVAILABLE COPY

1804/50854

**PRV**

PATENT- OCH REGISTRERINGSVERKET  
Patentavdelningen

MAILED 19 JUL 2004

WIPO

PCT

**Intyg  
Certificate**

Härmed intygas att bifogade kopior överensstämmer med de handlingar som ursprungligen ingivits till Patent- och registreringsverket i nedannämnda ansökan.

This is to certify that the annexed is a true copy of the documents as originally filed with the Patent- and Registration Office in connection with the following patent application.



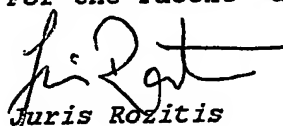
(71) Sökande Wouter van der Wijngaart Royal Institute of  
Applicant (s) Technology, Stockholm SE  
A Shane Ridgeway, What Cheer IA US  
Göran Stemme, Stockholm SE

(21) Patentansökningsnummer 0301637-5  
Patent application number

(86) Ingivningsdatum 2003-06-06  
Date of filing

Stockholm, 2004-07-12

För Patent- och registreringsverket  
For the Patent- and Registration Office

  
Juris Rozitis

Avgift  
Fee 170:-

**PRIORITY  
DOCUMENT**

SUBMITTED OR TRANSMITTED IN  
COMPLIANCE WITH RULE 17.1(a) OR (b)

STRICTLY CONFIDENTIAL STRICTLY CONFIDENTIAL STRICTLY CONFIDENTIAL STRICTLY CONFIDENTIAL STRICTLY CONFIDENTIAL

# **DESIGN AND EXPERIMENTAL STUDY FOR THE FABRICATION OF A MICROMACHINED IP CONVERTER**

**Author: Wouter van der Wijngaart**

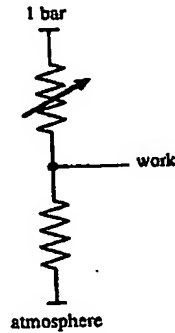
**Sponsor: Pondus Industries AB**

9  
5  
6  
4  
8  
8

## introduction:

### The basic configuration

The basic design of the IP converter is shown schematically in the figure below.



The work space is coupled to the supply pressure and vent (atmosphere) through controllable flow resistors. Either one or both flow resistors can be regulated.

The design study will focus on the actively changeable flow resistance.

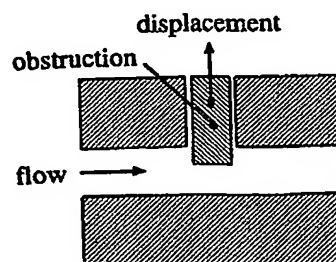
### The problem

Micromachined actuators have been included in many microsystem designs, including microvalves. However, either the actuator's stroke length or the force delivered by the actuator is limited. These effects are severely limiting the total performance for the majority of microvalve designs, where the actuator directly controls the movement of a boss. A small stroke length constitutes a high flow restriction between the boss and the valve seat, limiting the flow the valve can control. Large stroke lengths, on the other hand, limit the actuation force, and thus the pneumatic pressure that the valve can control. An increase of actuator size is space consuming, and thus often expensive.

### Low actuation force

A flow resistance can be seen as an obstruction in a flow channel or at a flow nozzle.

One of the main problems in microvalve design, is the fact that the flow obstruction has to counteract the pneumatic forces of the flow it controls. This however requires high actuation forces. We will therefore focus on designs where the flow obstruction movement is perpendicular to the gas flow. In this case, moving the obstruction requires virtually no energy. A schematic is shown in the figure below.



The obstruction is preferably a stiff structure, as it should not deform under the gas pressure forces.

### The stiction problem

In the Microsystems world, the downscaling of components has its specific consequences. Scaling down with a factor  $N$ , results in a downscaling of masses and volumes with  $N^3$  and of areas with  $N^2$ . This means that surface tension effects and tribological effects dominate in microsystems. It is therefore virtually impossible to use sliding structures in MST. Therefore, moving structures need to be "free-hanging".

This implies for any obstruction that moves perpendicular to the flow, there needs to be a small flow gap between the obstruction and the flow channel, as illustrated in the figure below. There will thus always exist some leak flow. Proper design however can minimise this leak flow.

low actuation power: Actuation force  $\perp$  Pneumatic force



Friction problem: Allow leaking !!!

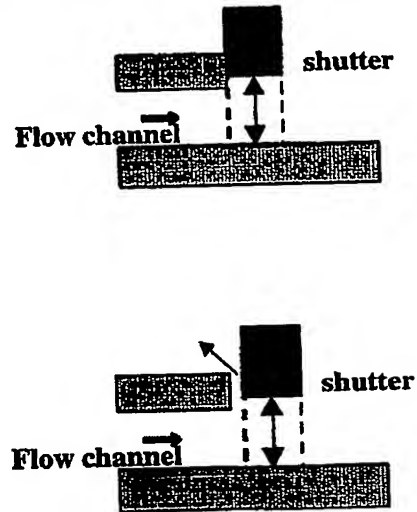
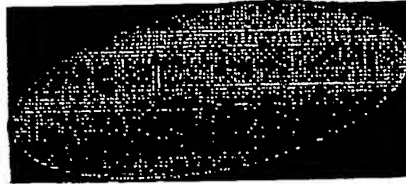


Figure. In designs where the obstruction moves perpendicular to the flow, a small gap between channel and obstruction is unavoidable.

### Flow channel dimension

A specific problem in microfluidics is the small cross-sectional flow-through area. As a thumb rule for design is that for higher pressures, the gas flow through an orifice is almost linear to the pressure drop. An orifice cross sectional area of  $1 \text{ mm}^2$  typically allows 4 l/min of gas flow per atmosphere. We will tackle this problem in our designs by keeping the small on-chip flow ducts as short as possible and trying to construct flow orifices rather than flow channels.

## Three basic designs



There exist three different basic designs for keeping the flow and the obstruction movement perpendicular to one another in (planar) micromachined valve structures.

### Design 1:

The gas flow  $Q_z$  is out-of-plane and the obstruction movement  $\Delta x$  in-plane

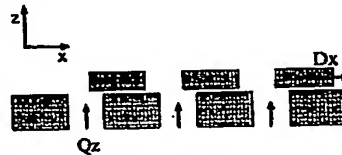
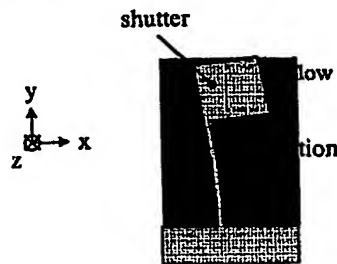


Figure. Cross sectional view design 1.

In this design, one or more nozzles can be closed with an obstruction plate. A similar design has been presented in [K. R. Williams & all, Lucas NovaSensor]. The reason to choose several nozzles is to diminish the obstruction stroke length  $Dx$ .



[K. R. Williams & all, Lucas NovaSensor]

Figure. Schematic of a valve as designed at Lucas Novasensor.

#### Proposed actuation:

- Thermal [cf. Lucas Novasensor]
- Comb drive (cf. appendix)

#### Fabrication issues:

- DRIE
- wafer-through inlet
- 2-wafer stack

### Design 2:

The gas flow  $Q_y$  is in-plane and the obstruction movement  $\Delta x$  in-plane but perpendicular to the gas flow

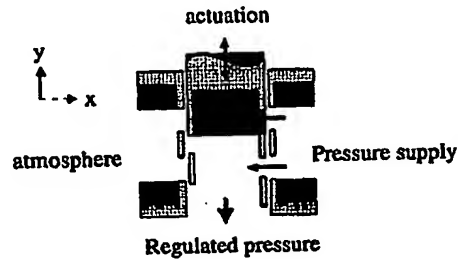


*Figure. Top view design 2.*

Proposed actuation:

- Thermal
- Comb drive

Proposed Fabrication:

- DRIE
- 3-wafer stack

### Design 3:

The gas flow  $Q_y$  is in-plane and the obstruction movement  $\Delta z$  out-of-plane.

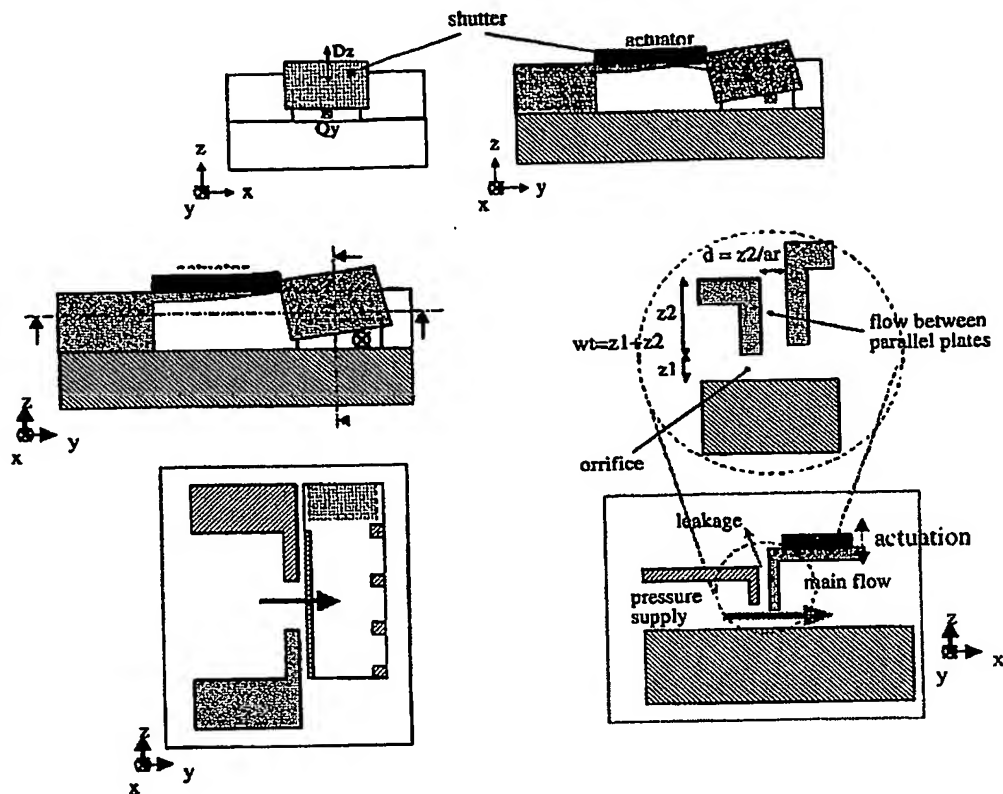


Figure. Cross sectional view design 3.

Proposed actuation:

- Thermal
- piezoelectric

Fabrication issues:

- DRIE
- 2-wafer stack

## The test device

The design 3 as depicted above was chosen for implementation in a first test device. The reason for this was the relative simplicity of fabrication.

### Theory

One can theoretically express the pressure-flow behaviour as follows.

$w$	The width of the flow nozzle.
$wt$	The total thickness of the top wafer
$z1$	The height of the flow nozzle
$a_r$	The aspect ration of the DRIE etch process
$P$	The supply pressure
$\mu$	The gas viscosity
$\rho$	The gas density
$Q$	The flow

The leak flow  $Q_{leak} = \frac{w(wt - z1)^2 P}{12 \cdot a_r^3 \cdot \mu}$  is modelled as a (laminar) poseuille flow between two parallel

plates. The workflow  $Q_{flow, max} = w \cdot z1 \cdot \sqrt{\frac{2P}{\rho}}$  is modelled as the flow through an orifice. This results in an

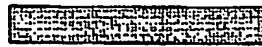
"leakage efficiency" of  $\frac{Q_{leak}}{Q_{flow, max}} = \frac{(wt - z1)^2}{12 \cdot a_r^3 \cdot \mu \cdot z1} \cdot \sqrt{\frac{\rho P}{2}}$ .

### Fabrication

A flow chart of the test device fabrication is shown in the figure below.



A 300µm thick silicon wafer is etched with DRIE.



The wafer is then oxidised.



The bottom oxide is patterned and masks the second DRIE step.



After removing all oxide, the structure is fusion bonded to an oxidised substrate.



Removing the oxide frees the obstruction, which is now only held by break-away-arm structures.



A piezo actuator is glued on top of the obstruction, the arms are broken off and a fluid opening is drilled. The structure is now ready for testing its pressure-flow characteristics.

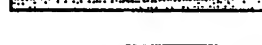


Figure. Schematic of the microfabrication process of the test structure.

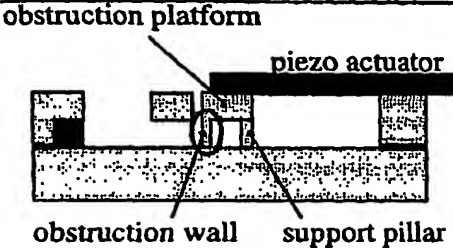
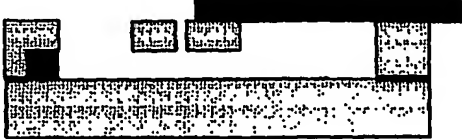
Copyright © 2000 and a  
Patent - PLS do not copy  
or modify in any way the picture.

Copyright © 2000 and a  
Patent - PLS do not copy  
or modify in any way the picture.

Figure. Two pictures of the test structures. The wafer contains three complete test structures and one test structure without tube connector. Wafer diameter is 10cm.

### Test results

The second DRIE step of the first series of test structures has been of low quality. The result is that the obstruction wall was etched away. This is illustrated in the figure below.

 <p>The structure as was intended. The obstruction wall blocks the flow, the obstruction platform allows the glueing of the piezo actuator, and the support pillars underneath the obstruction platform give it mechanical strength and stability.</p>	 <p>A fault during the etch process resulted that the obstruction wall and support pillars were removed. The obstruction platform therefore is very fragile before glueing to the piezo actuator.</p>
---	---

We were therefore forced to use the structure in an alternative scheme in order to get test results. This is illustrated in the figure below.



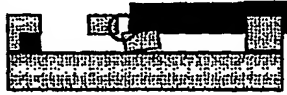
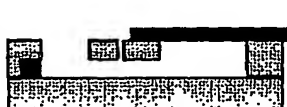
<i>The test structure as intended.</i>	<i>The alternative scheme</i>
<p>During non-actuation, the high flow resistance of the leak gap (indicated with a red circle) ensures low leak rates.</p>  <p>During open state, there is a low flow resistance.</p> 	<p>In order to close the valve, it has to be actuated with a negative voltage. The resistance of the gap is however poor compared to the intended design.</p> <p>When not actuated, the valve is in open state.</p>  

Figure. The construction failure forced us to use an alternative opening/closing scheme for the valve.

Despite the construction faults we were able to switch a flow between 650 and 500 sccm. These – for microsystems – very high flows occurred at a supply pressure of only a few kPa. This is roughly an improvement of 2 orders of magnitude compared to other micromachined valves.

### Conclusion

The test structure proved that

- Our new valve concept works
- (for microstructures) very high flows can be controlled
- Structures can be made with an easy microfabricational process
- Micromachining enables very small leak channels for the closed valve state (5µm).

STRICTLY CONFIDENTIAL STRICTLY CONFIDENTIAL STRICTLY CONFIDENTIAL STRICTLY CONFIDENTIAL

- The micromachined device area decrease has no fundamental theoretical limitations. Clever design and packaging can therefore help to minimise the cost of microfabrication, hereby alleviating one of the main limitations in microvalve technology.

## Appendix:

### In-plane obstruction actuation

Suitable in-plane actuation principles are:

- Electrostatic (comb drive):  
Relative large stroke length, weak force

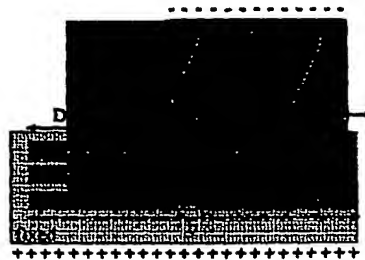


Figure. Top view on a comb drive

For a comb drive with an actuator area  $a*b$  (cf. figure) fabricated with DRIE, one can obtain a theoretical actuation force

$$F = a*b*eps*a_r/2*V^2 / 8*Dx*d$$

Where  $a_r$  is the aspect ratio of the DRIE process,  $d$  is the etch depth,  $eps$  is the absolute dielectric constant of air and  $V$  is the actuation voltage. This formula shows that a shallow comb drive allows a higher actuation force.

For design 1 however, a deep etch is preferred as this increases the stiffness of the obstruction.

A disadvantage of combdrives is that they are sensitive to particle contamination. The combdrive must inherently be connected to the outside world through a gas channel however (cf. The section on friction).

- Thermal:  
In-plane thermal actuation is used by the Lucas Novasensor design. In-plane thermal actuation exploits the fact that material expands when heated. Its features are relatively small stroke lengths, but high forces. Cantilevers however can circumvent the low-stroke problem.  
In general, thermal actuators are relatively slow and energy consuming however.

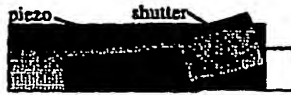
Actuation principles that are (too) complicated for in-plane fabrication are:

- Piezoelectric actuation
- Magnetic actuation

### Out-of-plane obstruction actuation

The problem with most out-of-plane actuation principles is their small stroke length. A typical upper limit is  $30\mu m$ . Suitable out-of-plane actuation principles are:

- Piezoelectric:  
A long piezo beam clamped at one side and with the obstruction element on the other side is an alternative used in the test structure.



- Thermal:

Here, bimorph elements are considered. Heating a bimorph results in a stress in the interface between both materials. Bimorphs give a high force-displacement product. Again, slow response and a high energy consumption can be expected.

- Magnetic:

Magnetic actuation has the advantage that there is no theoretical limitation on the stroke length. Also, if the obstruction is coupled to a spring system, a nearly linear I/P conversion is obtained. Integration of magnetic actuation with micromachined components can turn out difficult though.

Actuation principles that are not suitable are:

- electrostatic actuation:

Conventional static electrostatic actuators are "binary", i.e. or on, or of. There is only a small displacement range where the actuation voltage is "analogue". Besides, electrostatic actuation suffers from severe hysteresis. This makes electrostatic actuation undesirable from a control point of view.



PPV 03-06-05

CONFIDENTIAL

MST - S3/KTH 03-06-05

## X-Valve – A Miniaturised High Performance Valve

This document overviews a novel valve concept developed at MST - S3/KTH (<http://www.s3.kth.se/mst/>). The concept allows ultra-miniaturised components for high-flow, high-pressure applications.

### Design

The device is a silicon chip that regulates the flow from a pressurised supply nozzle, and is in fact a miniaturised knife gate valve. It uses a thermal bimorph actuator to control a "knife gate", a miniaturised silicon blade, which can perpendicularly move in front of a nozzle opening.

This design has the following unique features:

#### 1. Cross-flow:

Unlike most other microvalves presented, the flow direction and actuation direction are perpendicular to one another, i.e. the pneumatic static forces do not counteract the valve actuation, increasing the actuator stroke-length and reducing power consumption and actuator size. Note that the flow controlled by the valve is close to the physically allowed flow through such

#### 2. Out-of-plane nozzle:

Unlike all other microvalves presented, the gas supply nozzle is perpendicular to the wafer plane. This means that an increase of the required nozzle area does not directly require an increase of the silicon footprint area. The device is thus inherently more cost effective than all previously presented microvalves.

#### 3. Leak:

The price to pay... In order to avoid friction between the knife gate and the nozzle, a gap must remain, allowing leakage. We think this leakage could be reduced to about 1-2% of the main flow. The proceedings submitted to the Transducers '03 with the test results from the fabricated prototype for a similar valve design can be delivered.

### Valve control

The valve opening is either directly controlled linearly (amount of power delivered to the bimorph actuator) or controlled digitally. The latter design would split up a single knife gate into a series of 4-8 gates, each half the width of its neighbour. This allows 32-256 discrete flow settings for the valve using the same silicon footprint area.

### Device specification estimations

The below specifications give a general indication of an estimated typical performance, but depend strongly on the actual device dimensions.

- o Power consumption: a few 100mW?
- o Switching time: 10-100ms?
- o Flow: 3Nl/s @ when supplying 3 bar.
- o Maximum pressure (limited mainly by packaging techniques): several bar! (verified)
- o Microcomponent (silicon chip) size: 0.75\*8\*3 mm?

These values are up to two magnitude orders or more better in flow and pressure performance than existing pneumatic microcomponents. Silicon area consumption is a magnitude order lower, and power dissipation should be generally lower than comparable microvalves.

### Estimated Device Cost

The silicon core of the device is batch fabricated with silicon technology (based on microelectronics fabrication technology).

Micromachined part	Cost ~ consumed silicon area (3*8mm?) * amount/type of process steps (limited in the new concept)	30kr /device
Packaging	hard to tell, depends on the final design	20kr/device?
Total:		50kr/device?

Note: Packaging and mechanical stability issues mainly determine the feasible degree of miniaturisation.

**CONFIDENTIAL**

MST - S3/KTH 03-06-05

**Why microfabrication?**

Micromachining techniques allow:

- miniaturising the overall component size
- minimising and control of the leaky paths ( $\mu\text{m}$  size)
- batch fabrication
- integration of flow path, actuator and monitoring (flow or pressure sensor e.g.) on the same substrate and in the same fabrication sequence, thus reducing costs.

**Overall**

+ reduced device size + reduced production cost + high degree of controllability + control of high flow and large pressures + clogging insensitive	- in single valve configuration: leak flow
--	--



PRV 03-06-05

CONFIDENTIAL

MST – S3/KTH 03-06-05

## X-Valve – A Miniaturised High Performance Valve

This document overviews a novel valve concept developed at MST – S3/KTH (<http://www.s3.kth.se/mst/>). The concept allows ultra-miniaturised components for high-flow, high-pressure applications.

### Applications

The device is a packaged silicon chip with the functionality of an IP-converter (such as the PXA45 from Pondus Instruments) consists of a 3-port configuration:

- Port 1: pressure feed  $P_{supply}$
- Port 2: controlled pressure  $P_{work}$
- Port 3: vent  $P_{atm}$

### Technical design

The device uses a combination of two microvalve elements with thermal bimorph actuators.

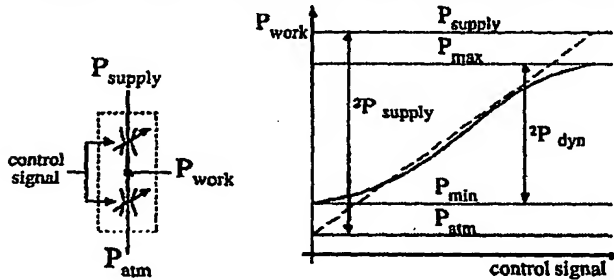


Figure 1. Functional representation of a pressure control element (left) and its pressure characteristics (right). The dashed line in the plot indicates the ideal behaviour, while the solid line indicates the actual performance.

A prototype of a single valve element was fabricated and tested (see figure 2). This element can be used as a stand-alone valve element if a high leak rate is allowed.

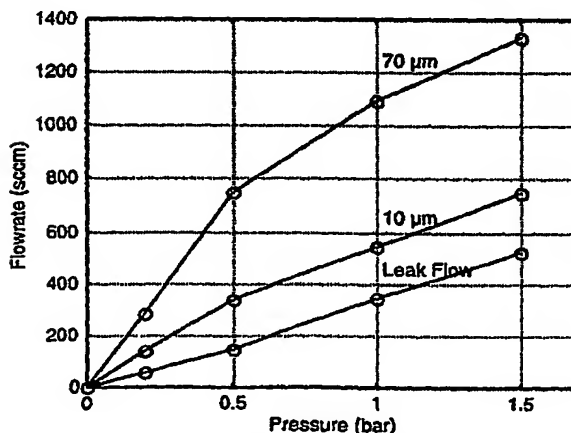


Figure 2. Measured flow-pressure performance of a single valve element prototype.

The leak rate of a single valve element determines the limitation to the relative dynamic work pressure range  $\Delta P_{dyn}$ . It was theoretically verified that for the measured leak rate of the microvalve prototype,

the relative dynamic work pressure range of a complete IP converter  $\frac{\Delta P_{dyn}}{\Delta P_{supply}} > 93\%$  for the complete pressure controller.

Due to patent pending issues, we do not wish to reveal the technical construction of the device.





**CONFIDENTIAL**

MST - S3/KTH 03-06-05

### Device specification estimations

The below specifications give a general indication of an estimated typical performance, but depend strongly on the actual device dimensions. Fault margins on the below values may be larger than a factor 2.

- Power consumption: (roughly linear to the power applied): a few 100mW? → Possibly powered directly via the control bus.
- Switching time: <10ms?
- Flow: several l/min (verified)
- Maximum pressure (limited mainly by packaging techniques): several bar! (verified)
- Microcomponent (silicon chip) size: 0.75\*3\*2 mm?

These values are up to two magnitude orders or more better in flow and pressure performance than existing pneumatic microcomponents. Silicon area consumption is a magnitude order lower, and power dissipation should be generally lower than comparable microvalves.

### Estimated Device Cost

The silicon core of the device is batch fabricated with silicon technology (based on microelectronics fabrication technology).

Micromachined part	Cost ~ consumed silicon area (3*2mm?) * amount/type of process steps (limited in the new concept)	€ 0.7/device
Packaging	hard to tell, depends on the final design	€ 0.3 /device?
Total:		€ 1 /device?

Note: There are no first-order limitations to the miniaturisation (cost). Packaging and mechanical stability issues mainly determine the feasible degree of miniaturisation.

### Why microfabrication?

Micromachining techniques allow:

- miniaturising the overall component size
- minimising and control of the leaky paths ( $\mu\text{m}$  size)
- batch fabrication
- integration of flow path, actuator and monitoring (flow or pressure sensor e.g.) on the same substrate and in the same fabrication sequence, thus reducing costs.

### Overall

+ reduced device size + reduced production cost + high degree of controllability + control of high flow and large pressures + clogging insensitive	- in single valve configuration: leak flow
--	--

# A MICROMACHINED KNIFE GATE VALVE FOR HIGH-FLOW PRESSURE REGULATION APPLICATIONS

Wouter van der Wijngaart, Anthony S. Ridgeway, Göran Stemme  
 Microsystem Technology, Department of Signals, Sensors, and Systems, Royal Institute of Technology,  
 SE-10044 Stockholm, Sweden.

## ABSTRACT

Cross-flow pressure regulating valve structures are attractive for high-flow pressure control applications due to the decreased actuation force required and the reduced device footprint area. A knife gate valve was fabricated, controlling a flow of 1.3 Nl/min at a supply pressure of 1.5 bar. The valve was microfabricated using deep reactive ion etching (DRIE) and silicon fusion bonding. The use of micromachined knife gate valves in pressure control systems enhances performance and cost savings can be realized.

## INTRODUCTION

One area of industry that holds potential for the introduction of microsystems is pressure regulation and control. Pressure controllers (also *E/P*-converters or *I/P*-converters where *E* stands for electrical, *I* for current and *P* for pressure), are basic elements in a vast number of industrial applications. Their basic function is to convert an electrical control signal into a work pressure  $P_{work}$ . Figure 1 shows a typical converter and its performance characteristics. The structure has three pneumatic ports: one supply port, indicated with index *supply*, one work port, indicated with index *work*, and one vent port, indicated with the indices *vent* or *atm* (this port is in most applications coupled to atmospheric pressure).

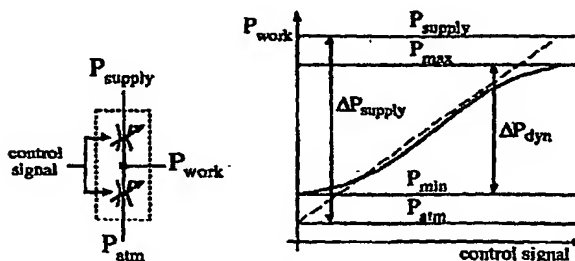


Figure 1. Functional representation of a pressure control element (left) and its pressure characteristics (right). The dashed line in the plot indicates the ideal behavior, while the solid line indicates a typical actual performance.

In the ideal case the valve would be able to control the work pressure over the entire range ( $\Delta P_{supply}$ ) between the atmospheric pressure ( $P_{atm}$ ) and the high supply pressure ( $P_{supply}$ ). In an actual case the valve controls a smaller dynamic range ( $\Delta P_{dyn}$ ), which is the difference between a maximum pressure ( $P_{max}$ ), slightly

below the supply pressure, and a minimum pressure ( $P_{min}$ ), slightly above the atmospheric pressure.

Pressure controllers would benefit from the cost advantages of microfabrication if performance can be maintained in terms of pressure and flow characteristics. Efforts have been made in the past to develop microvalves for pneumatic systems, however most cannot meet the demands of industrial use. Most previously reported microvalves are seat valves and utilize out-of-plane flow and actuation by means of a valve seat and boss [1-6]. The limited boss stroke-length severely limits their flow performance by the inherent restriction of the small flow ducts. Moreover, the static pneumatic force counteracts the valve actuation. To obtain a large flow rate and a high-pressure control performance with such valves the device footprint area must be increased accordingly. This decreases the device count per batch and thus increases manufacturing costs.

This paper introduces and proves a pressure control microvalve suitable for replacing large-scale valves. The novel device presented features an increased flow-pressure performance per device footprint area as compared to previously presented microvalves [1-7].

## THEORY AND DESIGN

A knife gate microvalve (Figure 2) has been developed which circumvents the above performance drawbacks.

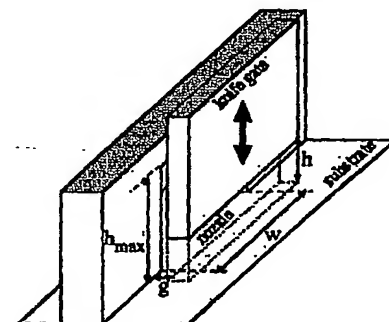


Figure 2. The knife gate valve principle.

The valve gate moves perpendicular to the flow and the static pneumatic force (hence the name *cross-flow valve* or *X-Valve*). The static pressure and valve actuation are not counteracting one another, thereby reducing the required actuator force and size. Moreover, the X-Valve features in-plane gas flow and out-of-plane gate

displacement. Unlike all previously reported microvalves the nozzle area is perpendicular to the wafer plane; therefore the footprint area consumed by the device is independent from its pressure and flow performance. The X-Valve thus allows control of larger flow and higher pressure with a more compact design.

The X-Valve requires spacing between the gate and the nozzle to avoid friction and therefore leaks in the closed state. However, in pressure controller applications this is of minor importance. Leakage influences the controller's static pneumatic energy loss and reduces the dynamic pressure range of the device

$$\Delta P_{dyn} = P_{max} - P_{min} < \Delta P_{supply} = P_{supply} - P_{atm} \quad (\text{Figure 1}).$$

For lower Mach numbers and for device dimensions of interest, frictional losses in the leak gap are negligible. This results from the low ratio of the gate-nozzle spacing ( $g$ ) over leak path length and the smoothness of the (micromachined) surface of the leak path [8]. If at high Mach numbers frictional losses do occur, they would further decrease the leakage. Both the main flow and leak flow can thus be modeled as isentropic flow in a sudden expansion, in which the mass-flow

$$(1) \quad \dot{m} \propto A_{cs} P_{supply} \left( \frac{P_{atm}}{P_{supply}} \right)^{1/\gamma} \sqrt{\left( \frac{P_{supply}}{P_{atm}} \right)^{1-1/\gamma} - 1}$$

with  $A_{cs}$  being the minimal cross-sectional area of the flow path and  $\gamma$  the gas specific heat ratio [8,9]. The leak rate can then be quantified as

$$(2) \quad \eta = \frac{\dot{m}_{leak}}{\dot{m}_{max}} = \frac{A_{cs, leak}}{A_{cs, max}} = \frac{(2h_{max} + w) \cdot g}{h_{max} \cdot w} = \frac{g}{h_{max}}$$

for  $w \gg h_{max}$ , with  $h_{max}$  the nozzle height,  $w$  the nozzle width, and the indices *leak* and *max* referring to the conditions and dimensions at the gate-nozzle spacing and the maximum nozzle opening, respectively.

For a pressure controller as illustrated in Figure 1 containing two identical control valves with leak rate  $\eta$ ,  $P_{min}$  and  $P_{max}$  can be calculated using the mass flow continuity equation

$$(3) \quad \dot{m}_{supply} = \dot{m}_{work} + \dot{m}_{atm} = \dot{m}_{atm}$$

at zero work flow.  $P_{work} = P_{min}$  if the vent port is open and the supply port is closed, in which case  $A_{cs, supply} = \eta \cdot A_{cs, vent}$ , respectively  $P_{work} = P_{max}$  if the vent port is closed and the supply port is open, in which case  $A_{cs, vent} = \eta \cdot A_{cs, supply}$ .  $P_{min}$  and  $P_{max}$  can thus be calculated as the respective solutions of the equations

$$(4) \quad \eta \cdot P_{supply} \left( \frac{P_{min}}{P_{supply}} \right)^{1/\gamma} \sqrt{\left( \frac{P_{supply}}{P_{min}} \right)^{1-1/\gamma} - 1} = P_{min} \left( \frac{P_{atm}}{P_{min}} \right)^{1/\gamma} \sqrt{\left( \frac{P_{min}}{P_{atm}} \right)^{1-1/\gamma} - 1}$$

and

$$(5) \quad P_{supply} \left( \frac{P_{max}}{P_{supply}} \right)^{1/\gamma} \sqrt{\left( \frac{P_{supply}}{P_{max}} \right)^{1-1/\gamma} - 1} = \eta \cdot P_{max} \left( \frac{P_{atm}}{P_{max}} \right)^{1/\gamma} \sqrt{\left( \frac{P_{max}}{P_{atm}} \right)^{1-1/\gamma} - 1}$$

Graphically solving these equations for 1 bar (relative) supply pressure shows that for a leak rate  $\eta = 20\%$ ,  $P_{max} = 0.9815$  bar and  $P_{min} = 0.0376$  bar, resulting in a pressure range  $\frac{\Delta P_{dyn}}{\Delta P_{supply}} = 94.4\%$ .

## FABRICATION

A non-optimized demonstrator structure, requiring minimum processing, was fabricated using silicon bulk micromachining and silicon fusion bonding and is shown in Figure 3.

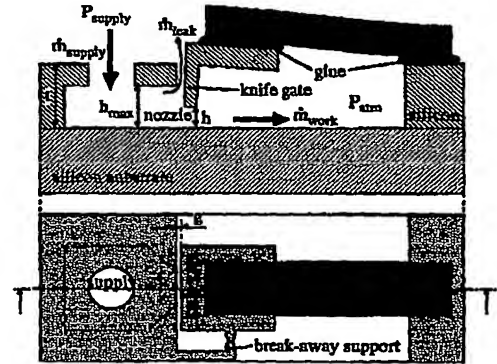


Figure 3. Simplified drawing of the demonstrator X-Valve structure.

Figure 4 shows the processing steps used to fabricate the structure. To start, a 200  $\mu\text{m}$  thick double-side-polished silicon wafer is spin coated with resist and patterned. The front-side of the device is DRIE etched to a depth of 130  $\mu\text{m}$  (Figure 4a). Next, thermal oxide 1  $\mu\text{m}$  thick is grown (Figure 4b). The resist is then removed using oxygen plasma. The backside is patterned and DRIE etched to a depth of  $h_{max} = 70$   $\mu\text{m}$  defining the maximum gate opening (Figure 4c,d). The resist is again stripped using oxygen plasma and the oxide is removed using a buffered HF solution releasing a fall-out structure (Figure 4e). The 200  $\mu\text{m}$  machined wafer is silicon fusion bonded with a 500  $\mu\text{m}$  single-side-polished wafer (Figure 4f). After drilling an inlet opening, a fluid connector is attached as well as a piezoelectric bimorph actuator using a two-part adhesive epoxy. The structure, supporting the knife gate during manufacturing, is now removed by breaking (Figure 4g). Note that the use of fall-out structures and the opening of the fluid connector with a mechanical drill were chosen in this fabrication scheme to

minimize the exposed silicon area during the first DRIE step and thus optimize the etch quality.

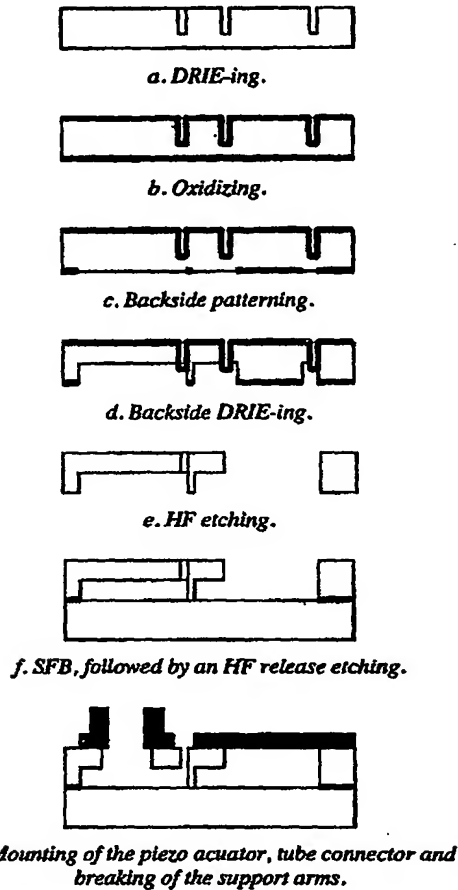


Figure 4. Simplified drawings, illustration the processing steps for the fabrication of the demonstrator X-Valve structure.

## EXPERIMENTAL RESULTS

A demonstrator structure with dimensions  $g = 10\mu\text{m}$ ,  $h_{\text{max}} = 70\mu\text{m}$ , and  $w = 2\text{mm}$  (Figure 2) was fabricated and tested. Note that the  $10\mu\text{m}$  gate-nozzle spacing did not hinder the movement of the gate.

The demonstrator structure was tested by measuring the flow rate through the device at varying supply pressure and gate opening height. The inlet of the structure was supplied with pressures of 0.2, 0.5, 1, and 1.5 bar. At each of these inlet pressures the flow rate was measured for different gate opening heights. Figures 5 and 6 show the flow measurements of the demonstrator structure as functions of the valve gate opening and supply pressure, respectively.

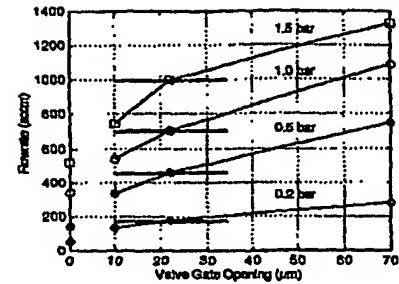


Figure 5. The measured valve flow rate  $Q_{\text{valve}}$  versus the gate opening  $h$  at different supply pressures  $P_{\text{supply}}$ .

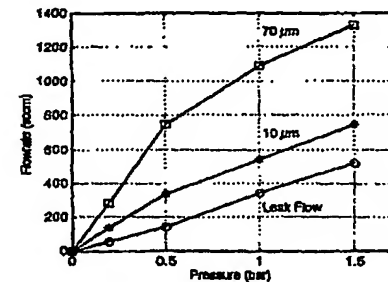


Figure 6. The measured valve flow rate  $Q_{\text{valve}}$  versus the supply pressure  $P_{\text{supply}}$  at different gate openings  $h$ .

During fabrication, some  $10\mu\text{m}$  sized silicon structures, used for improved fabrication characteristics, detached and became fixed under the knife gate, which in turn would not allow the valve to fully close. These structures create a minimum gate opening of exactly  $10\mu\text{m}$  when the knife gate is closed and attribute to the according flow measurement, shown in Figures 5 and 6. The zero gate opening flow, i.e. the pure leak flow, was measured using an identical device with a non-adjustable gate, fabricated for the purpose of leak flow testing. In the other measurements, the gate opening height was adjusted by applying voltage to the piezoelectric bimorph element. The gate opening was determined visually with a microscope. The uncertainty in the gate opening measurements gives rise to the large errors, indicated with bars in Figure 5 for the flow measurement at  $22\mu\text{m}$  gate opening.

The leak flow through the valve at 0.5 bar was approximately  $0.15\text{ NI/min}$ , which is about 19.5% of the measured maximum flow. This valve performance makes the structure a viable candidate for pressure controller applications. Moreover, the pressure-flow performance of the demonstrator valve,  $1.3\text{ NI/min}$  at 1.5 bar supply pressure, is a factor of two better than previously reported values for microvalves.

## COMPLETE MICROFABRICATED IP-CONVERTER

With the proven performance of the X-Valve concept a complete microfabricated IP-converter design is

## A Micromachined Knife Gate Valve for High-Flow Pressure Regulation Applications

Wouter van der Wijngaart, Anthony S. Ridgeway, Göran Stemme

Royal Institute of Technology, Department of Signals, Sensors and Systems - Microsystem Technology,  
Stockholm, Sweden

This abstract presents a new cross-flow microvalve concept, named X-Valve, for use in high-flow pressure controllers. A test structure was fabricated and successfully tested. The X-valve concept features an increased flow-pressure performance per device footprint area as compared to previously presented microvalves [1,2].

Pressure controllers (also *E/P-converters* or *I/P-converters*), are basic elements in a vast number of industrial applications. Their basic function is to convert an electrical control signal into a pressure output  $P_{work}$  (see Figure 1). Most previously reported microvalves are seat valves. They are severely limited in their flow performance by the inherent restriction of microscale flow ducts and in their pressure control by the static pressure forces counteracting the valve actuation.

We developed a knife gate microvalve (see Figure 2), which circumvents the above performance drawbacks. The valve gate moves perpendicular to the flow and the static pneumatic force (hence the name cross-flow-valve or X-Valve). The static pressure and valve actuation are therefore not counteracting one another, reducing the required actuator force and size. Moreover, the X-Valve features in-plane gas flow and out-of-plane gate displacement. Unlike all previously reported microvalves, the nozzle area is perpendicular to the wafer plane, and therefore the footprint area consumed by the device is independent from its pressure and flow performance. The X-Valve thus allows control of larger flow and higher pressure with a more compact design.

The X-Valve requires spacing between the gate and the nozzle to avoid friction and therefore leaks in the closed state. However, in pressure controller applications this is of minor importance. Leakage influences the controller's static pneumatic energy loss, and reduces the dynamic pressure range of the device  $\Delta P_{dyn} = P_{max} - P_{min} < \Delta P_{supply} = P_{supply} - P_{atm}$  (see Figure 1). It was theoretically verified that for lower Mach numbers and for device dimensions of interest, frictional losses in the leak gap are negligible. (High Mach number frictional losses further decrease leakage). Both the main flow and leak flow can be modeled as isentropic flow in a sudden expansion, in which the mass-flow  $\dot{m} \propto A_{cs} P_{supply} \left( \frac{P_{atm}}{P_{supply}} \right)^{1/\gamma} \left[ \left( \frac{P_{supply}}{P_{atm}} \right)^{1/\gamma} - 1 \right]$  with  $A_{cs}$

being the nozzle cross-sectional area and  $\gamma$  the gas specific heat ratio [3,4]. The leak rate can then be quantified as  $\eta = \frac{Q_{leak}}{Q_{max}} = \frac{A_{leak}}{A_{max}} = \frac{(2h+w) \cdot g}{h \cdot w} = \frac{g}{h}$  for  $w \gg h$ , with  $g$  being the gate-nozzle spacing,  $h$  the gate opening, and  $w$  the nozzle width. Further, it was theoretically verified that for a leak rate  $\eta=20\%$  the relative dynamic work pressure range  $\frac{\Delta P_{dyn}}{\Delta P_{supply}} > 93\%$  for a pressure controller (see Figure 1).

A demonstrator structure (see Figure 3) was fabricated using DRIE and silicon fusion bonding. The device dimensions measure  $w=2\text{mm}$ ,  $h=70\mu\text{m}$  and  $g=10\mu\text{m}$ , and the device is actuated with a glued piezoelectric bimorph. The device was successfully tested, and the flow-pressure and flow-gate opening performance are shown in Figures 4 and 5. Note that the cross-flow gate actuator means that the flow can be controlled gradually through the gate position  $h$ .

At a supply pressure  $P_{supply}=50\text{kPa}$ , the flow can be switched between  $Q_{leak}=146\text{sccm}$  and  $Q_{max}=750\text{sccm}$  ( $\eta=19.5\%$ ). This pressure-flow performance is a factor of two better than previously reported values for microvalves.

A novel compact microvalve design with large flow-pressure characteristics for pressure controller applications was successfully demonstrated.

### Contact Author:

Wouter van der Wijngaart

Royal Institute of Technology, Department of Signals, Sensors and Systems, Microsystem Technology, SE-100 44 Stockholm, Sweden

Ph: +46 8 790 6613 Fax: +46 8 10 08 58 Email: Wouter.Wijngaart@s3.kth.se

# References

- [1] Mark J. Zdeblick, R. Anderson, J. Jankowski, B. Kline-Schoder, L. Christel, R. Miles, and W. Weber, "Thermopneumatically actuated microvalves and integrated electro-fluidic circuits," in *Technical digest of the Solid-state sensor and actuator workshop*, Hilton Head, South Carolina, USA, 1994, pp. 251-255.
- [2] Kirt. R. Williams, N. Maluf, E. Fuller, R. Barron, D. Jaeggi, B. van Drieënhuizen, "A silicon microvalve for the proportional control of fluids," in *Proc. 10<sup>th</sup> International conference on solid-state actuators* (Transducers '99), Sendai, Japan, June, 1999, pp. 1804-1807.
- [3] A. K. Henning, "A compact, pressure- and structure-based gas flow model for microvalves." In *Proceedings, Materials and Device Characterization in Micromachining*, International Society for Optical Engineering, Bellingham, WA, 2000; Y. Vladimirovsky and P. J. Coane, eds., volume 4175.
- [4] Frank M. White, *Fluid mechanics*. New York, NY: McGraw-Hill, 4<sup>th</sup> edition, 1999.

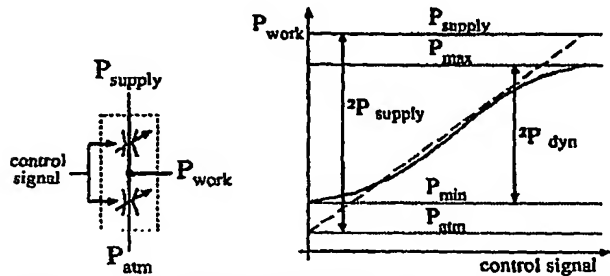


Figure 1. Functional representation of a pressure control element (left) and its pressure characteristics (right). The dashed line in the plot indicates the ideal behavior, while the solid line indicates the actual performance.

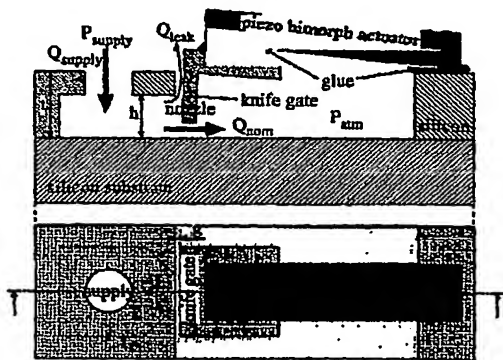


Figure 3. Illustration of the demonstrator X-Valve structure.

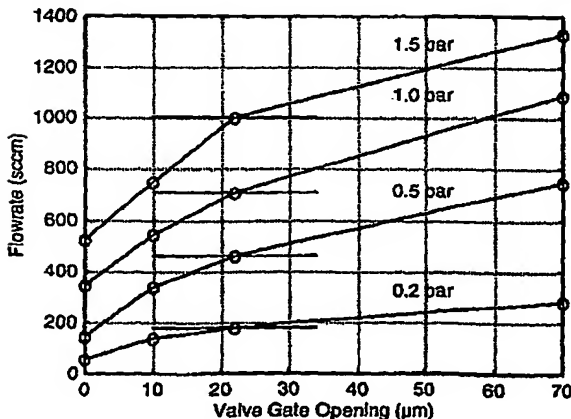


Figure 4. The measured valve flow rate  $Q_{supply}$  versus the gate opening  $h$  at different supply pressures  $P_{supply}$ .

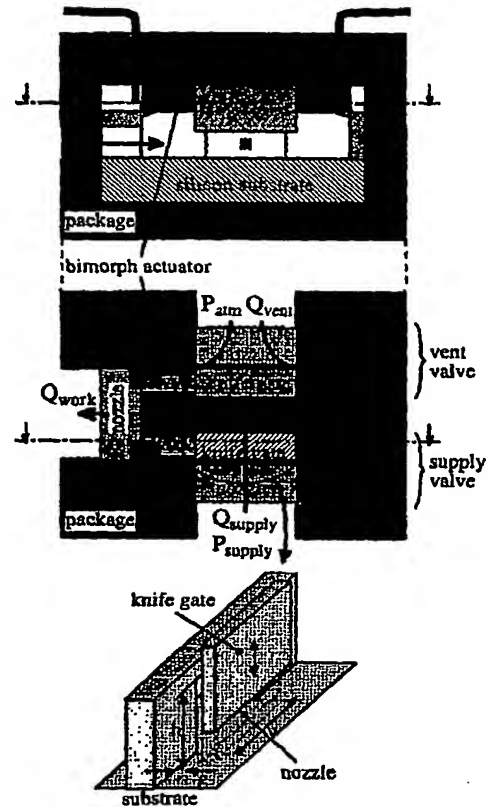


Figure 2. Schematic of a micro pressure controller with two X-Valves (not to scale).

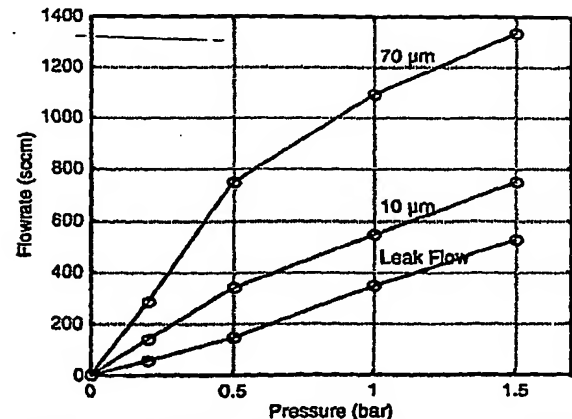
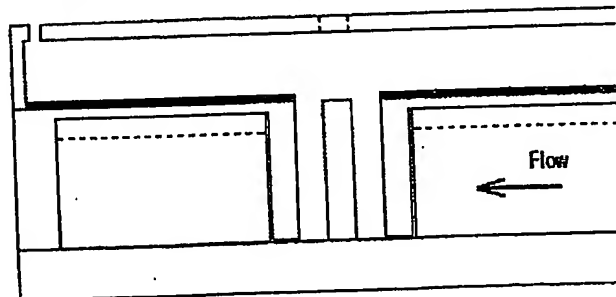
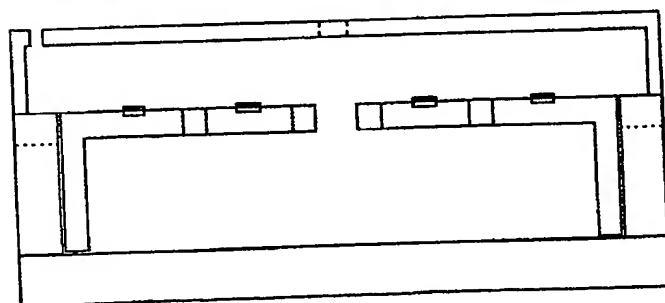
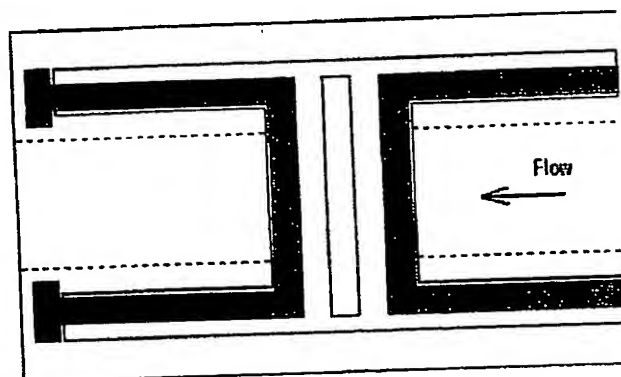
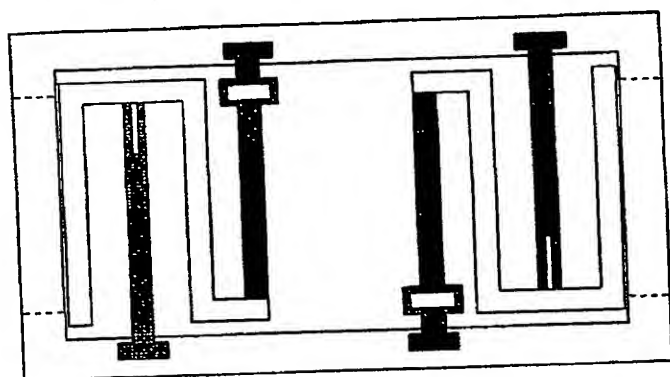
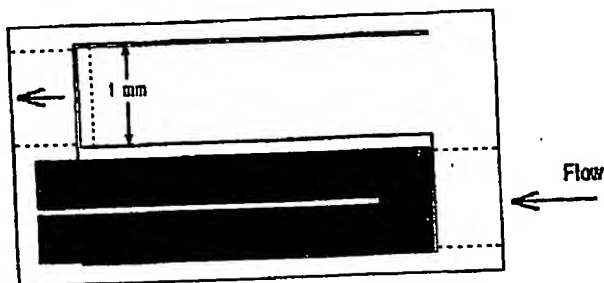
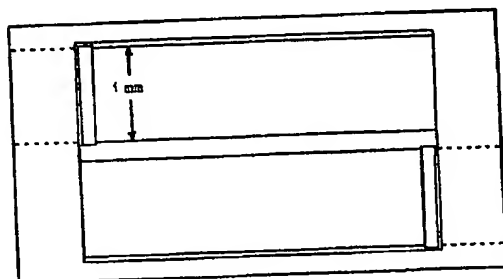
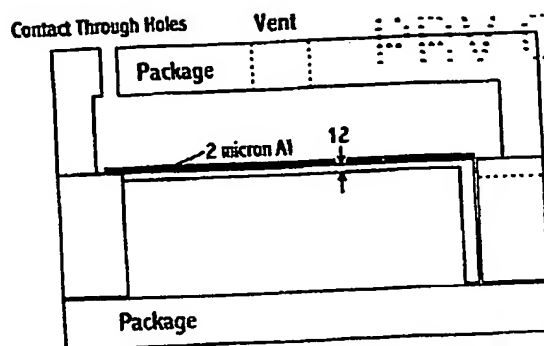
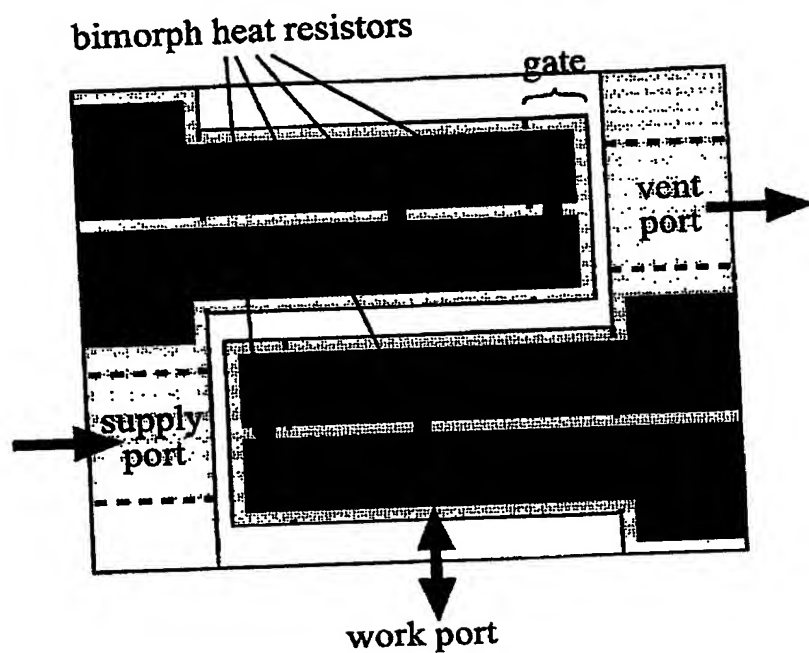
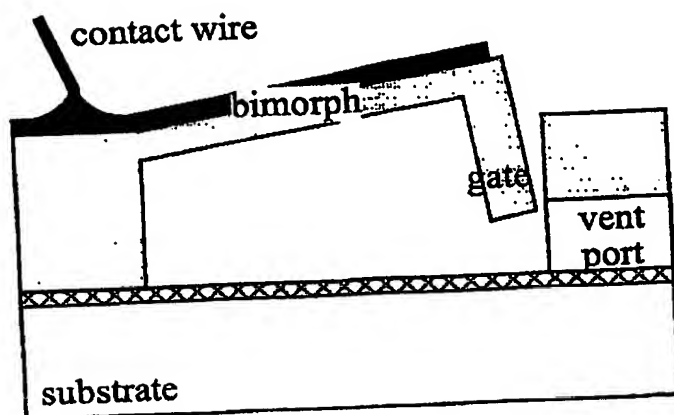


Figure 5. The measured valve flow rate  $Q_{supply}$  versus the supply pressure  $P_{supply}$  at different gate openings  $h$ .

1994-05-05

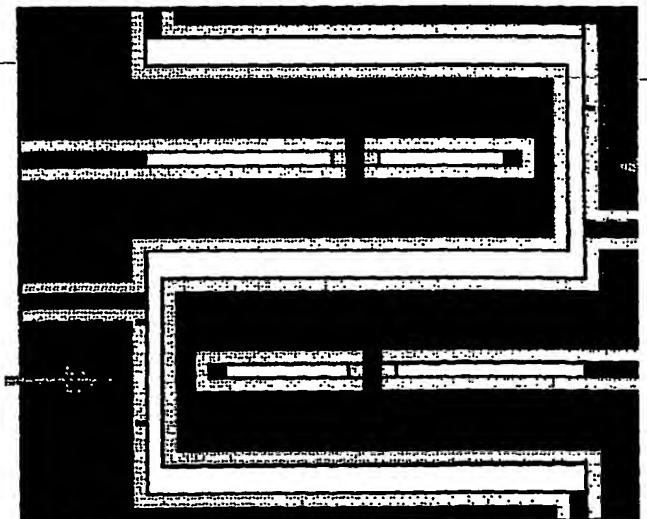
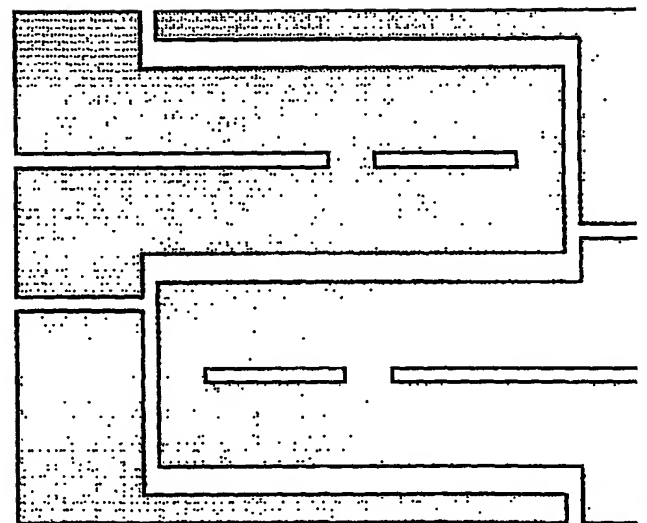
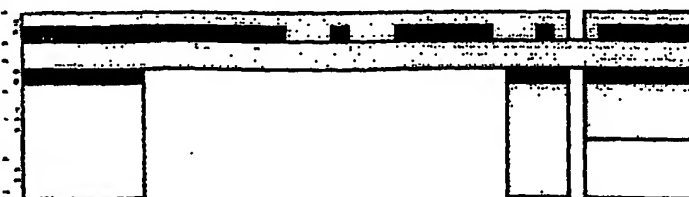
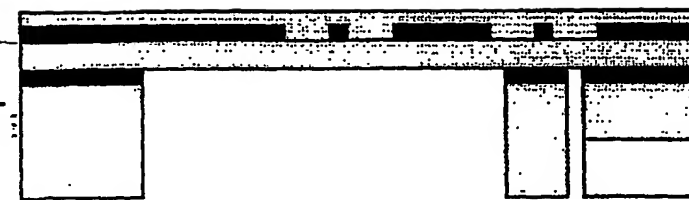
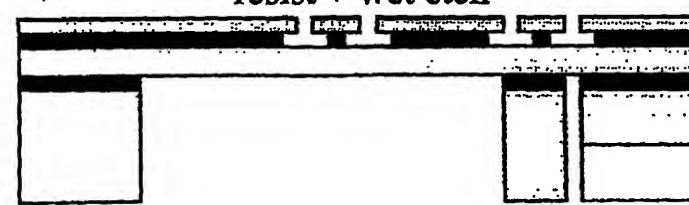
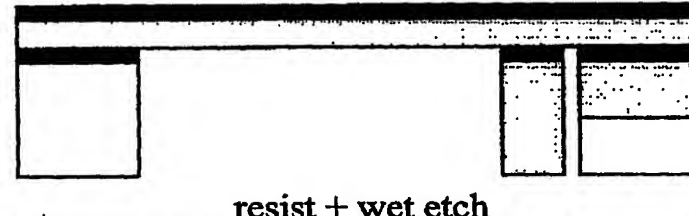
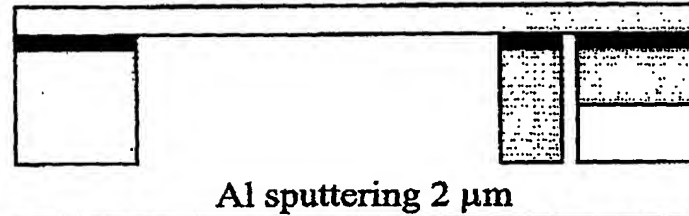
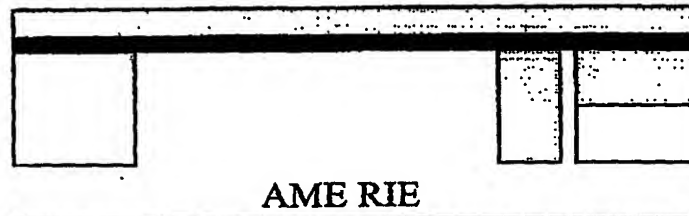
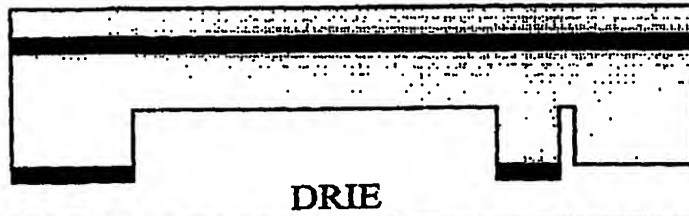
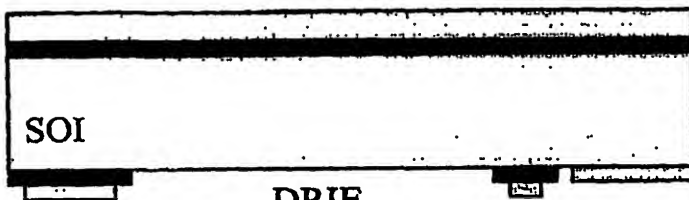


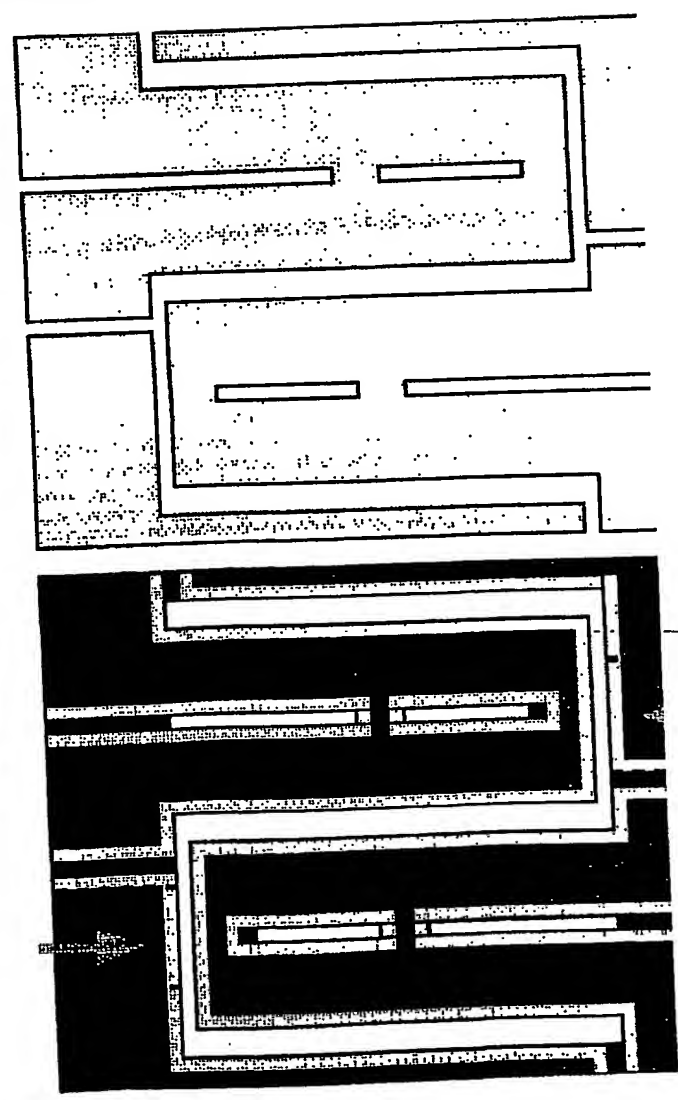
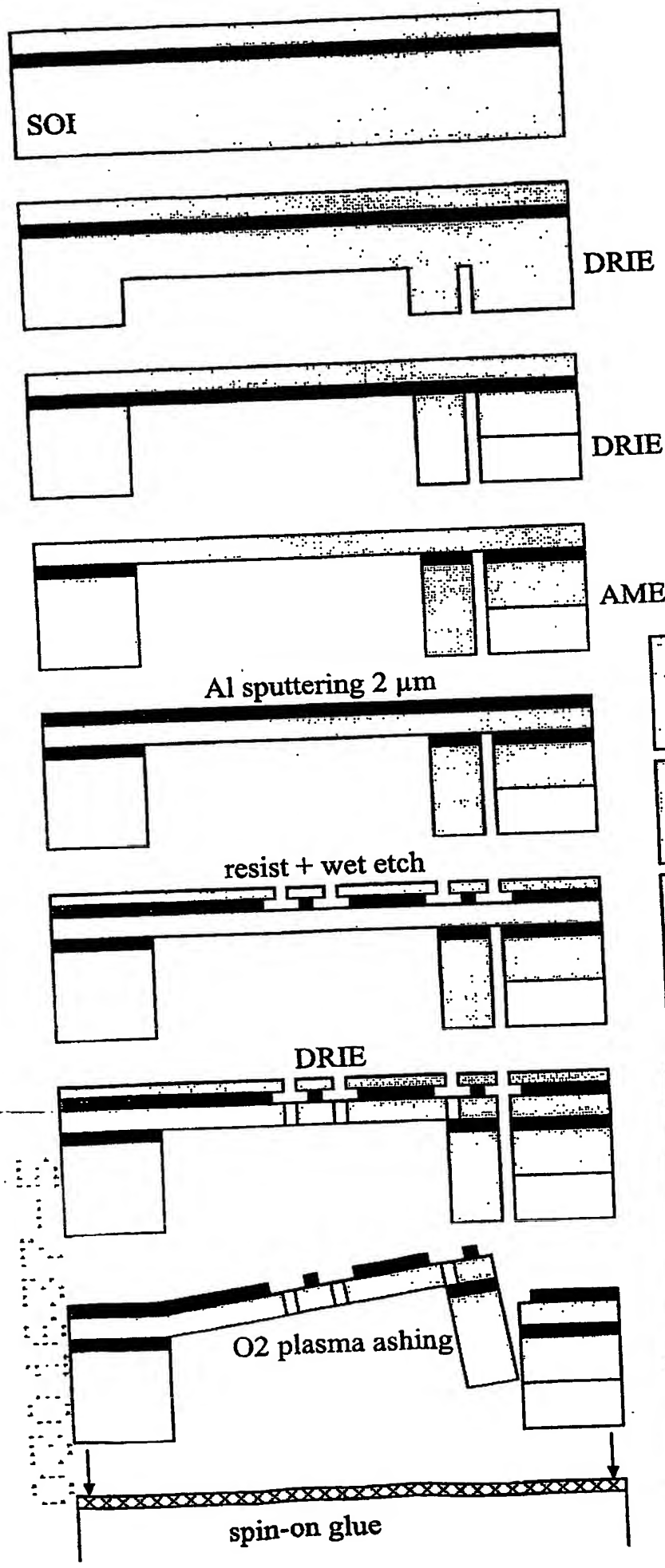
4659



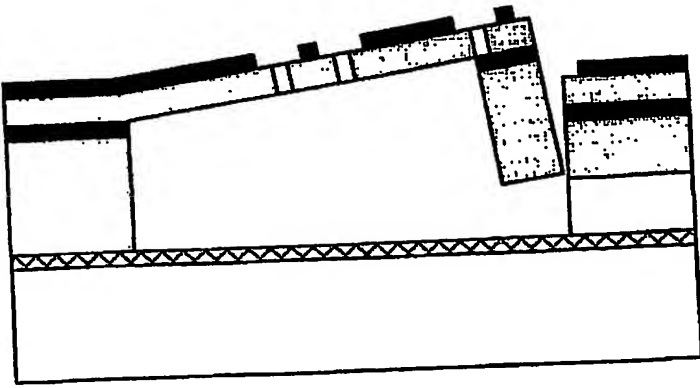


PRV 030000





PRV 03.06.98



PRV 03.06.98

**X-Valve Process Plan**  
**Version 1**  
**15/5/2003**

**Processes Required**

1. Thermal Oxide Growth
2. Lithography
3. Aluminum sputtering and wet etching
4. DRIE

**Processing Steps**

1. Oxidize Wafers – 1  $\mu$ m thickness
  - a. Furnace B-7; @1100 °C – 160 minutes
2. Remove Topside Oxide Using
  - a. AME (or Tape and Buffered HF)
3. Sputter Aluminum - 2  $\mu$ m Thickness on Topside
4. Pattern Aluminum with Mask 3
  - a. HMDS (Optional)
  - b. OPTITRAC - Coat
  - c. KARL SUSS
  - d. OPTITRAC – Develop
  - e. Hard Bake
5. Wet Etch Aluminum – W1215
6. Remove Resist Mask
  - a. TEGAL or TEPLA
7. Coat Topside with Thick Protective Resist (AC4562 or SBR220) – Thick Enough to Withstand 2 Resist Mask Strips
  - a. HMDS (Optional)
  - b. OPTITRAC - Coat
  - c. KARL SUSS
  - d. OPTITRAC – Develop
  - e. Hard Bake
8. Pattern Bottomside Oxide with Mask 1
  - a. HMDS
  - b. OPTITRAC - Coat
  - c. KARL SUSS
  - d. OPTITRAC – Develop
  - e. Hard Bake
9. Etch Oxide Mask
  - a. AME
10. Remove Bottomside Resist Mask
  - a. TEGAL or TEPLA
11. Pattern Bottomside with Mask 2
  - a. HMDS

- b. OPTITRAC - Coat
  - c. KARL SUSS
  - d. OPTITRAC - Develop
  - e. Hard Bake
- 12. DRIE Bottomside to a Depth of Approximately 200  $\mu\text{m}$ 
  - a. ICP
- 13. Strip Bottomside Resist Mask
  - a. TEGAL or TEPLA
- 14. DRIE Bottomside to Buried Oxide Layer (Approximately 200  $\mu\text{m}$ )
  - a. ICP
- 15. Coat Bottomside with Thick Protective Resist
  - a. Use Manual Spinner and Tape
  - b. Hard Bake
- 16. Strip Topside Protective Resist
  - a. TEGAL or TEPLA
- 17. Pattern Topside with Mask 4
  - a. HMDS
  - b. OPTITRAC - Coat
  - c. KARL SUSS
  - d. OPTITRAC - Develop
  - e. Hard Bake
- 18. DRIE Topside to Release Beams and Fall-Out Structures
- 19. Remove All Resist (Resist Masks and Protective Resist Layers)
  - a. TEGAL or TEPLA

proposed that combines two X-Valves in a fully packaged and operable device. Figure 7 gives the details of the makeup of the micromachined core of the device and its basic functions.

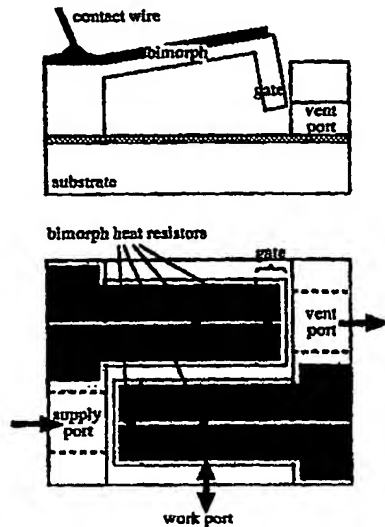


Figure 7. Schematic cross-sectional and top view of a micro pressure controller with two X-Valves (not to scale).

The pneumatic connectors will be integrated in the sides of the chip package. Actuation for the valves is provided by cantilevered thermal bimorphs. One X-Valve provides flow regulation at the supply port while a second X-Valve provides flow regulation at the vent port. A third port is used for the work flow ( $Q_{work}$ ). With the supply port closed and vent port open, the work area is evacuated. With the supply fully open and the vent closed the maximum work pressure is generated. The two X-Valves can be actuated either together or independently to achieve the work flow required.

## CONCLUSIONS AND FUTURE WORK

We have presented a novel microvalve concept for pressure control applications. The design is the key element in a truly miniaturized micromachined high-performance pneumatic control element. A demonstrator structure was fabricated using DRIE and silicon fusion bonding. The demonstrator structure is actuated with a glued piezoelectric bimorph. The device was successfully tested and the flow-pressure and flow-gate opening performance were measured. The valve flow can be controlled gradually through the gate position. The pressure-flow performance of the demonstrator valve presented is a factor of two better than previously reported values for microvalves. Future work focuses on the fabrication of a complete micromachined pressure controller with integrated thermoelectric bimorph actuators.

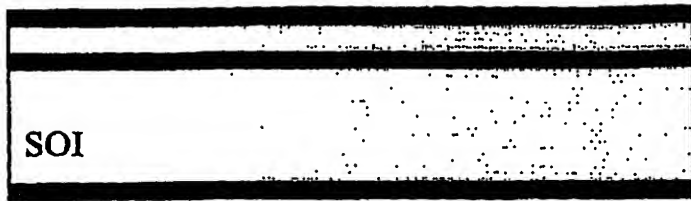
## ACKNOWLEDGEMENTS

The authors would like to thank Pondus Instruments AB, Stockholm, Sweden for sponsoring this research.

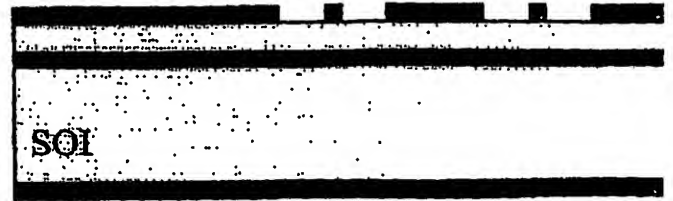
## REFERENCES

- [1] M. Huff, J. Gilbert, and M. Schmidt, "Flow characteristics of a pressure balanced microvalve," *Proc. 7th International Conference on Solid State Actuators (Transducers)*, Yokohama, Japan, June, 1993, pp. 98-101.
- [2] H. Jerman, "Electrically-activated normally closed diaphragm valves," *Journal of Micromechanics and Microengineering*, vol. 4, pp. 210-216, 1994.
- [3] S. Messner, M. Muller, V. Burger, J. Schaible, H. Sandmaier, and R. Zengerle, "A normally-closed, bimetallically actuated 3-way microvalve for pneumatic applications," *Proc. 11th International Workshop on Micro Mechanical Systems*, Heidelberg, 1998, pp. 159-164.
- [4] P. W. Barth, C.C. Beatty, L.A. Field, J.W. Baker, and G.B. Gordon, "A robust normally closed silicon microvalve," *Technical Digest of the Solid-State Sensor and Actuator Workshop*, Hilton Head, SC, USA, 1994, pp. 248-250.
- [5] P.W. Barth, "Silicon microvalves for gas flow control," *Proc. 8th International Conference on Solid-State Sensors and Actuators and Eurosensors IX*, Stockholm, Sweden, 1995, vol. 2, pp. 276-279.
- [6] Mark J. Zdeblick, R. Anderson, J. Jankowski, B. Kline-Schoder, L. Christel, R. Miles, and W. Weber, "Thermopneumatically actuated microvalves and integrated electro-fluidic circuits," in *Technical Digest of the Solid-State Sensor and Actuator Workshop*, Hilton Head, South Carolina, USA, 1994, pp. 251-255.
- [7] Kirt. R. Williams, N. Maluf, E. Fuller, R. Barron, D. Jaeggi, B. van Drieënhuizen, "A silicon microvalve for the proportional control of fluids," in *Proc. 10th International Conference on Solid-State Actuators (Transducers '99)*, Sendai, Japan, June, 1999, pp. 1804-1807.
- [8] Frank M. White, *Fluid mechanics*. New York, NY: McGraw-Hill, 4th edition, 1999.
- [9] A. K. Henning, "A compact, pressure- and structure-based gas flow model for microvalves." In *Proceedings, Materials and Device Characterization in Micromachining*, International Society for Optical Engineering, Bellingham, WA, 2000; Y. Vladimirovsky and P. J. Coane, eds., volume 4175.

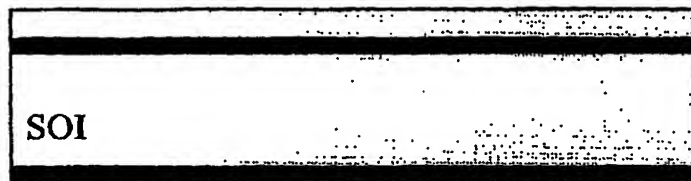
**Oxidize**



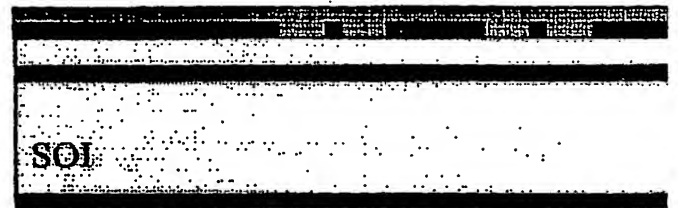
**Remove Resist Mask**



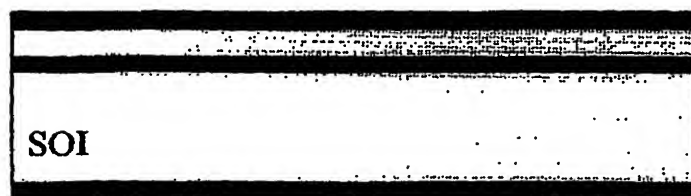
**Remove Topside Oxide**



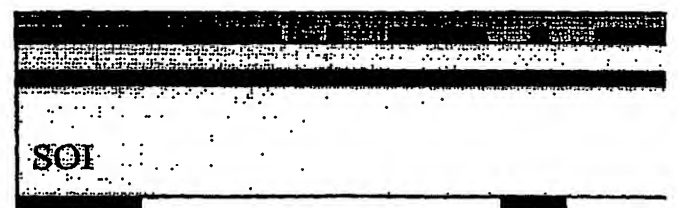
**Coat Topside Protective Resist**



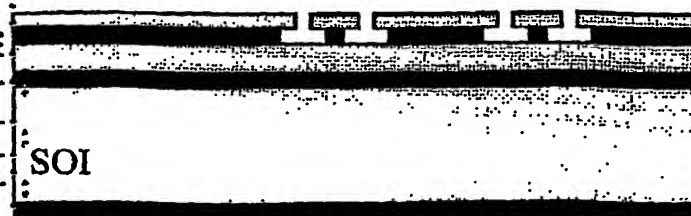
**Sputter Aluminum**



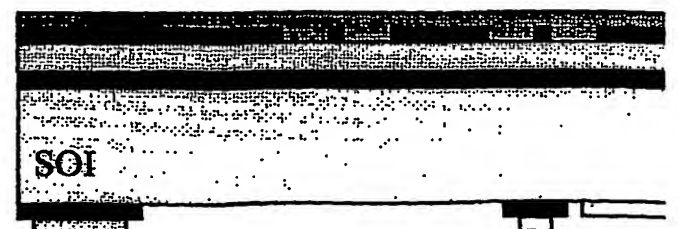
**Pattern Bottomside Oxide**



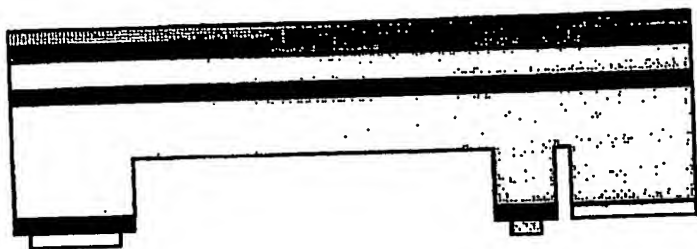
**Pattern and Wet Etch Aluminum**



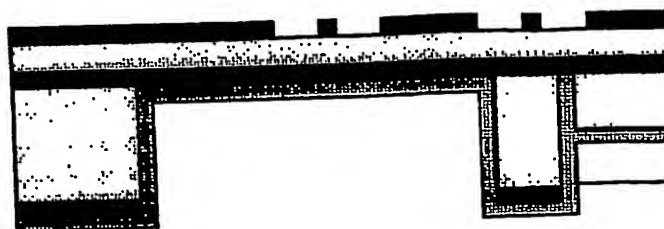
**Pattern Bottomside w/ Resist Ma**



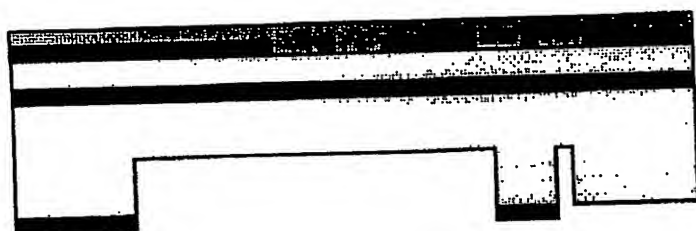
**DRIE**



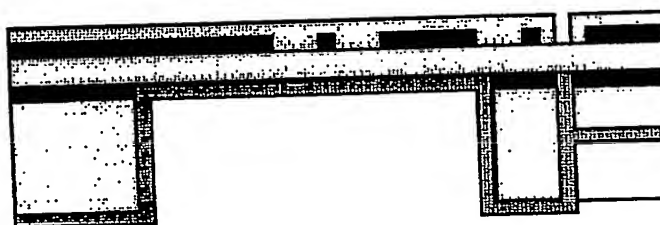
**Strip Topside Protective Resist**



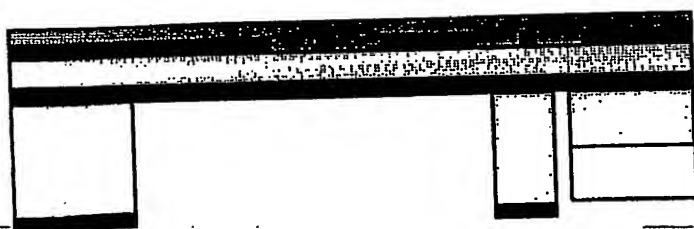
**Strip Resist Mask**



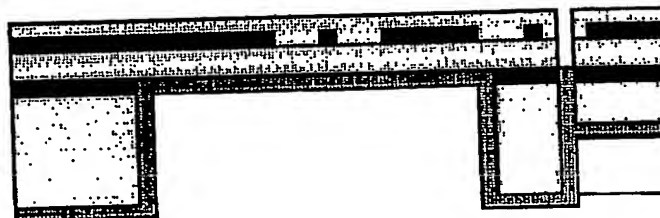
**Pattern Topside**



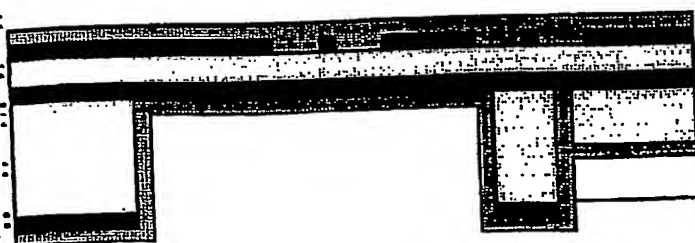
**DRIE**



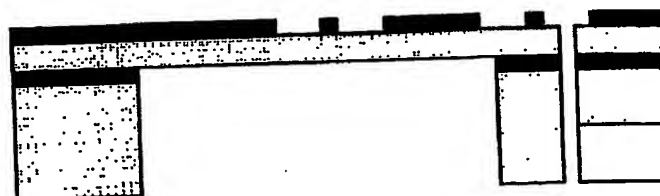
**DRIE**



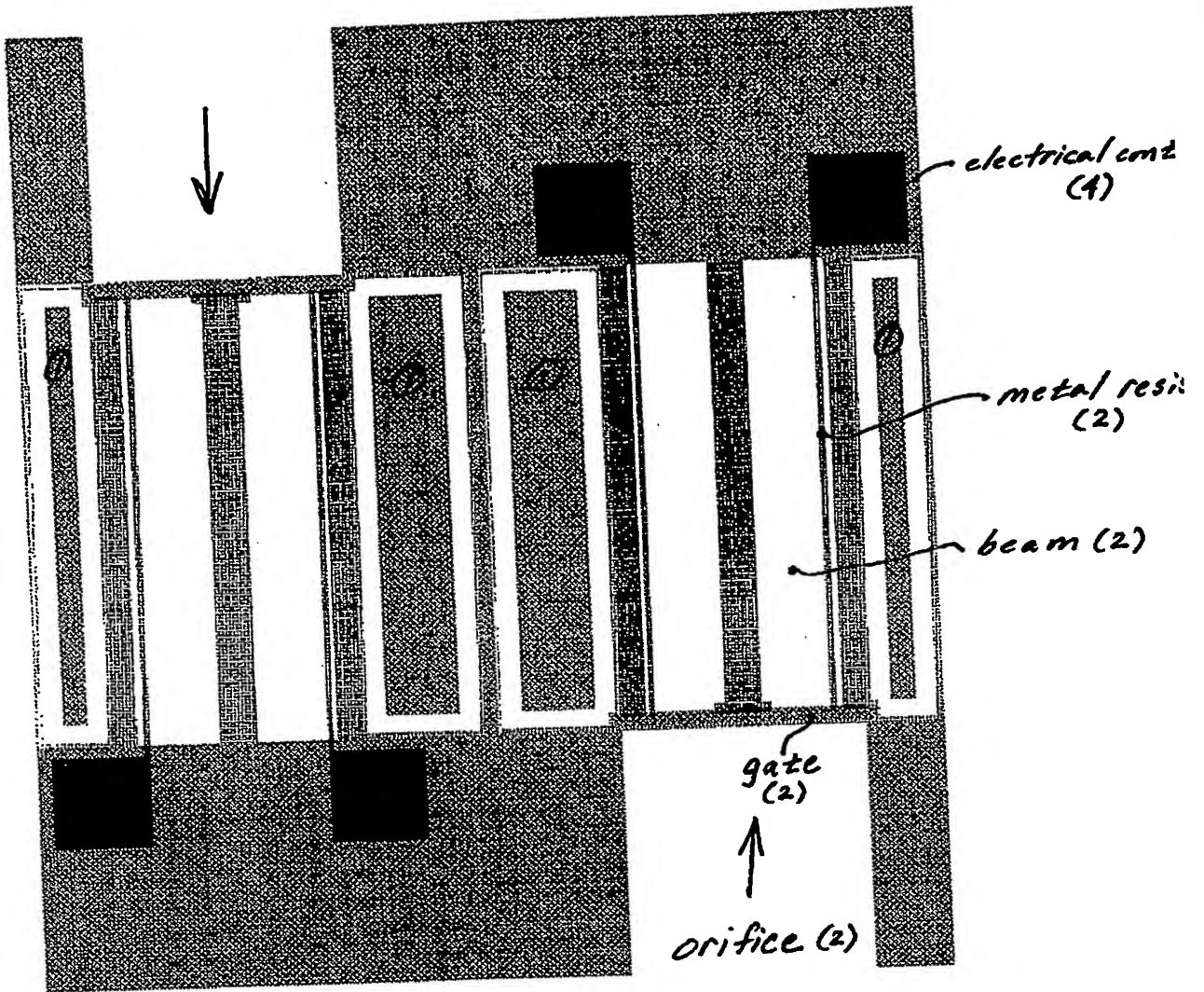
**Coat Bottomside Protective Resist**



**Remove All Resist**







① fallout structure

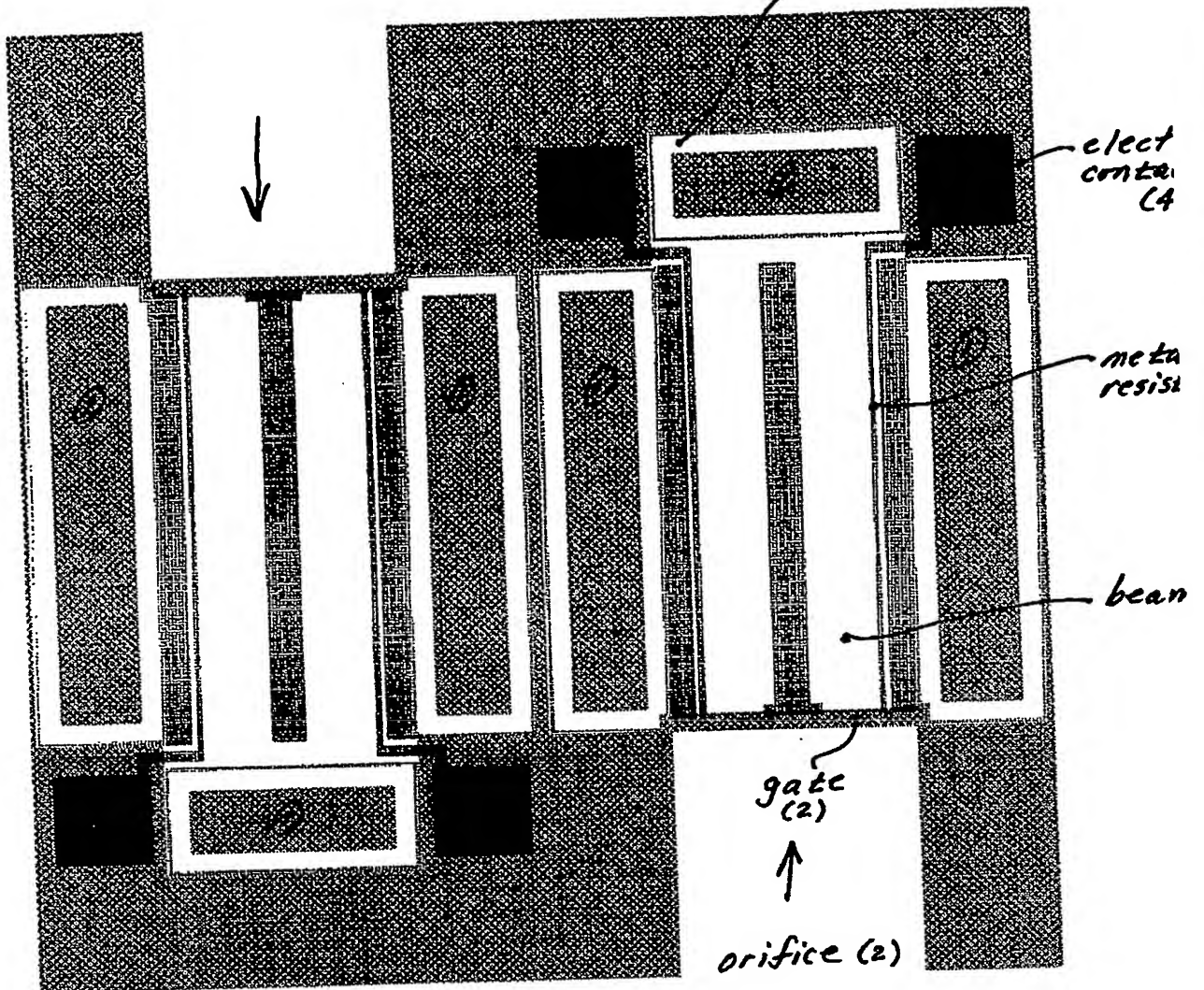
→ flow

4  
5  
6  
7  
8  
9



PRV 03-06-08

flow-through orifice 1

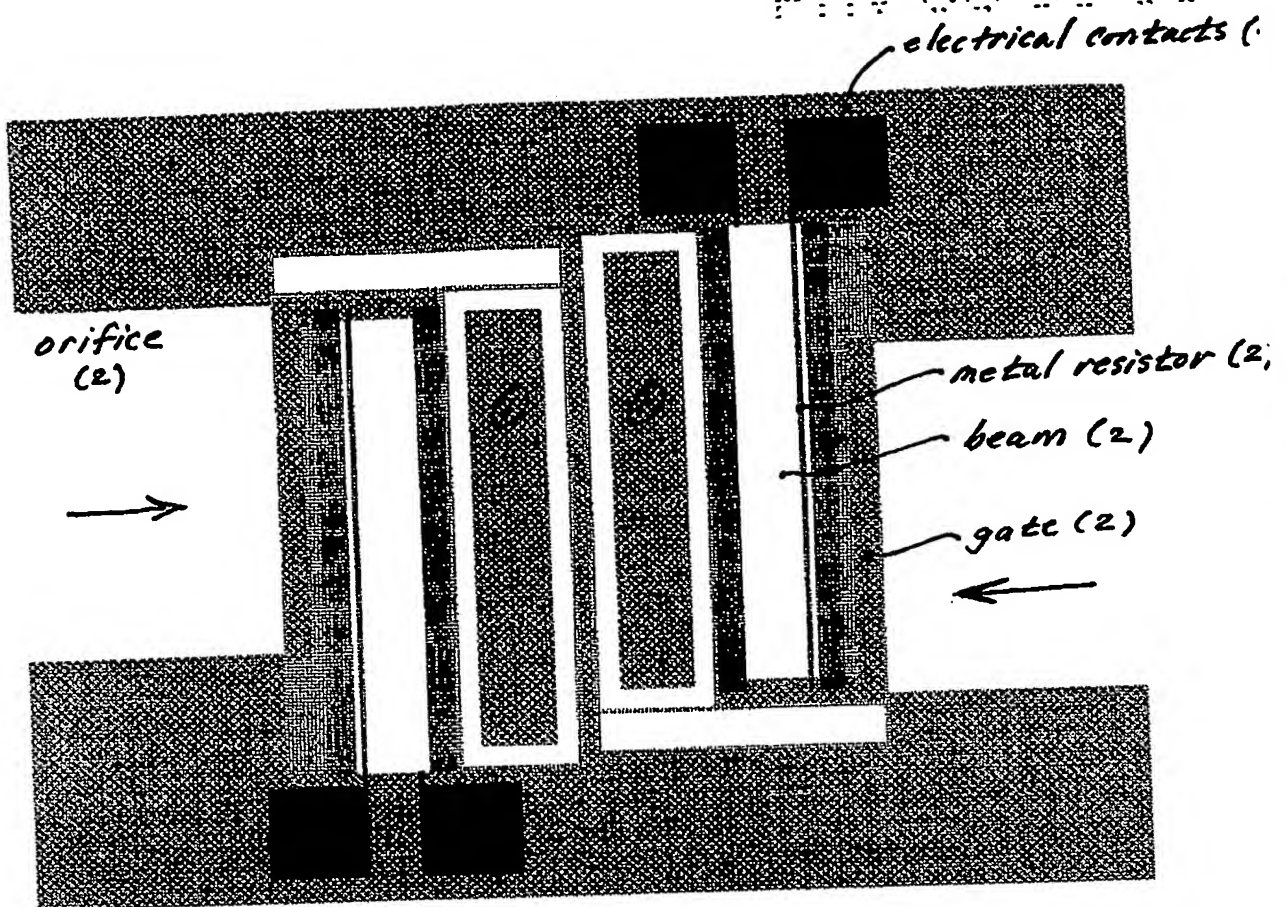


① fallout structure

→ flow.

03-06-08

PRV 03-06-06

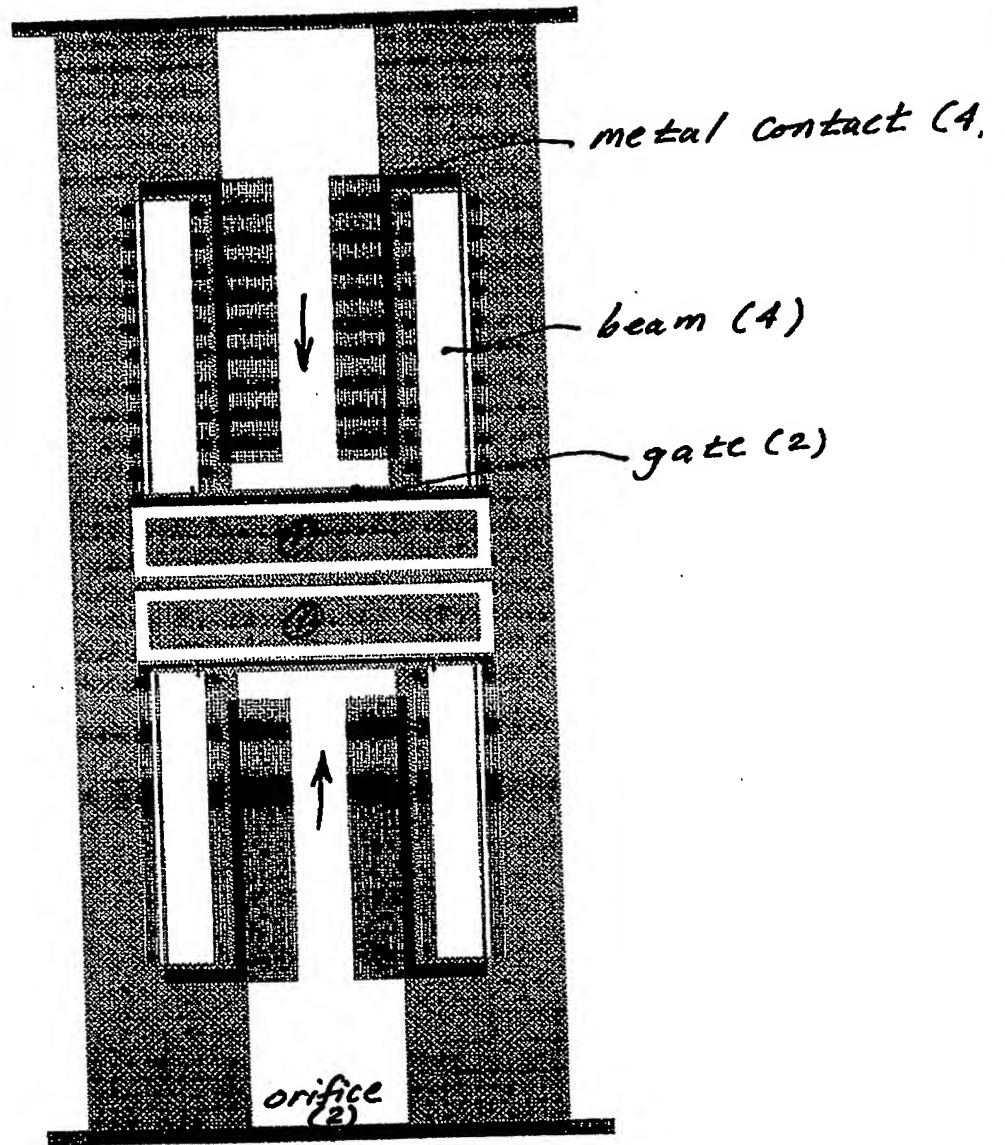


① fallout structure

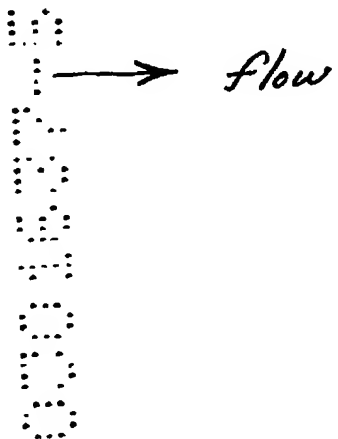
→ flow

03-06-06

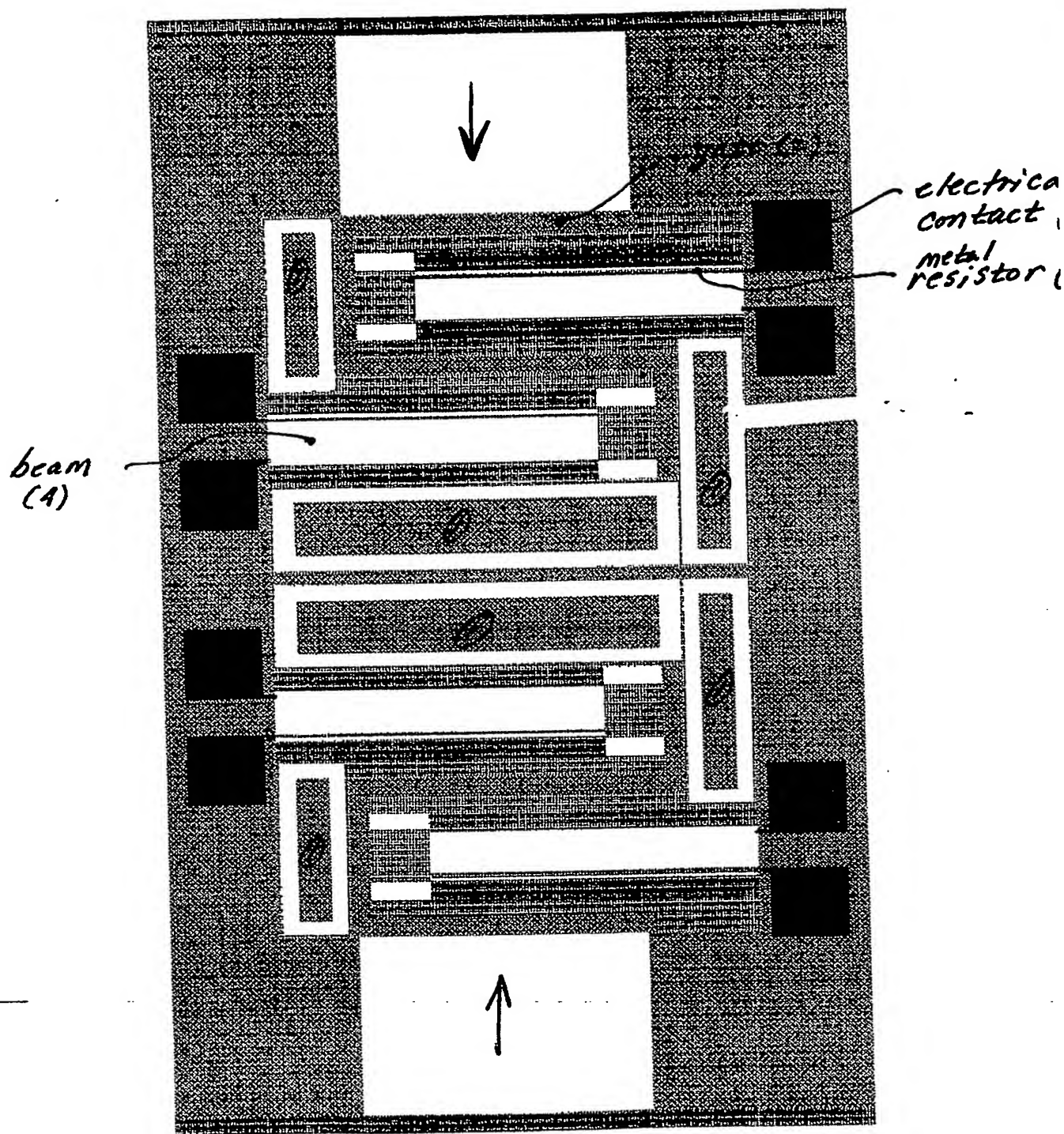




— ① fallout structure

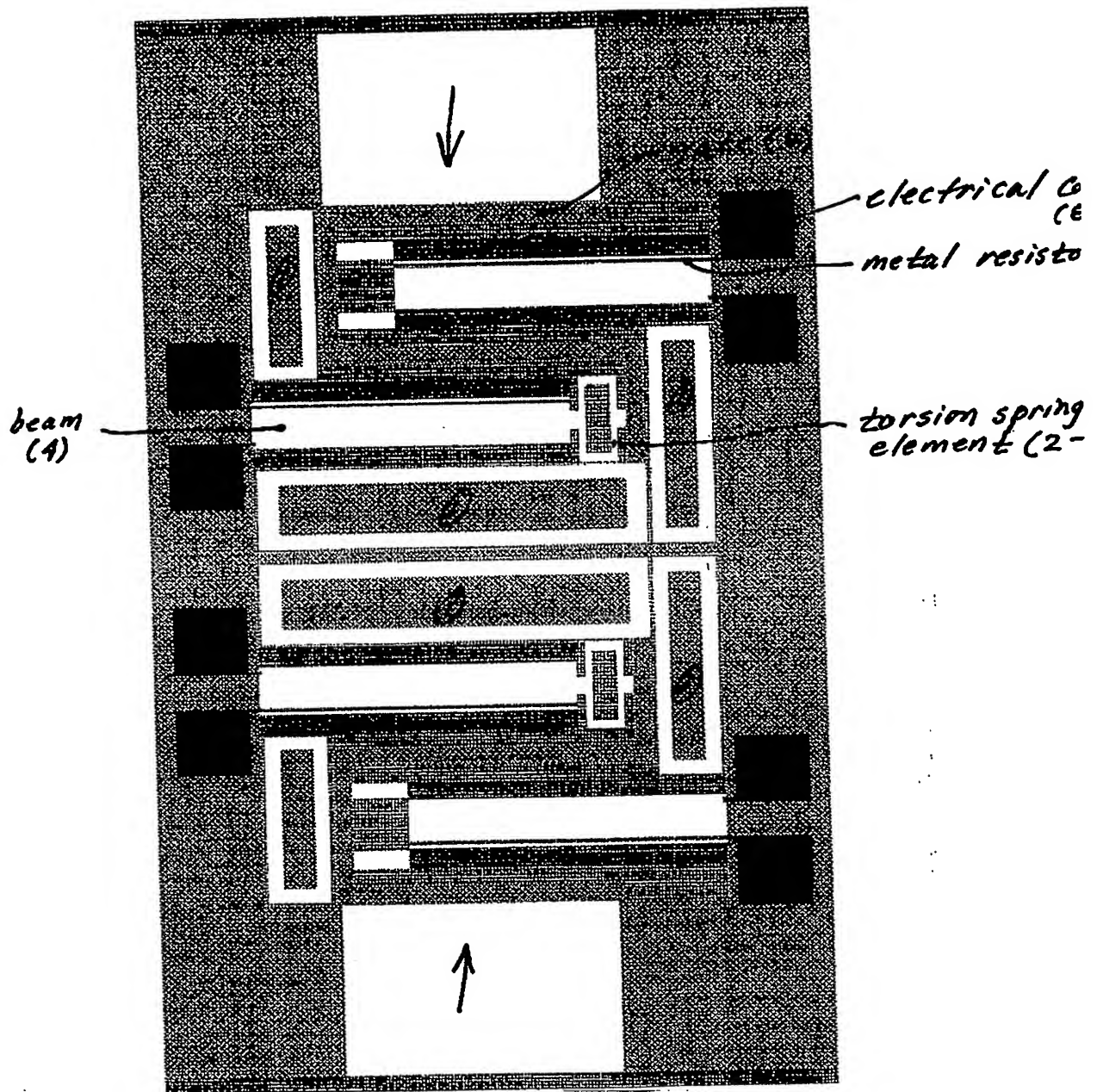




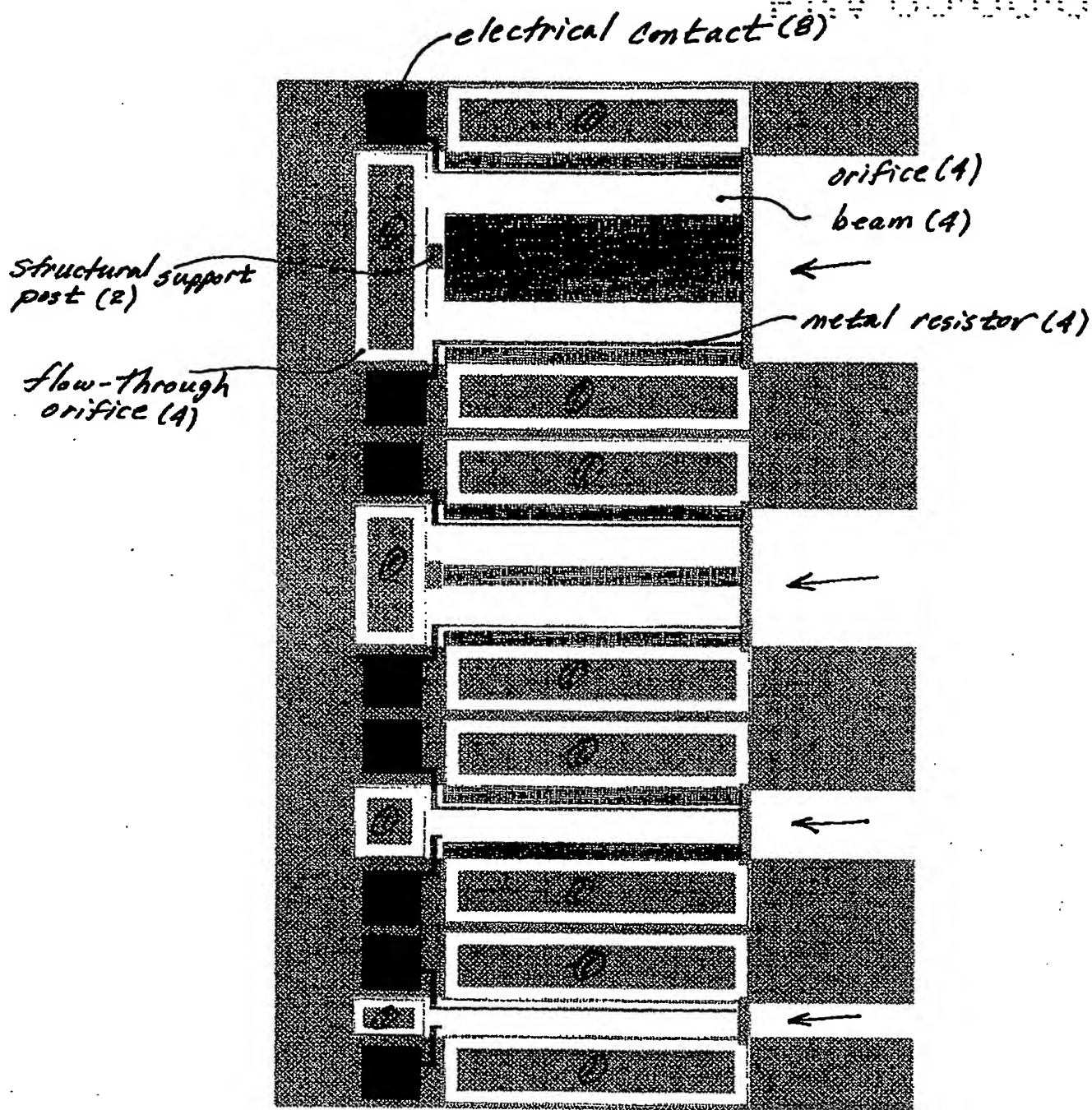


① fallout structure

→ flow







① fallout structure

→ flow

**This Page is Inserted by IFW Indexing and Scanning  
Operations and is not part of the Official Record**

**BEST AVAILABLE IMAGES**

Defective images within this document are accurate representations of the original documents submitted by the applicant.

Defects in the images include but are not limited to the items checked:

- ☐ BLACK BORDERS
- ☐ IMAGE CUT OFF AT TOP, BOTTOM OR SIDES
- ☐ FADED TEXT OR DRAWING
- ☐ BLURRED OR ILLEGIBLE TEXT OR DRAWING
- ☐ SKEWED/SLANTED IMAGES
- ☒ COLOR OR BLACK AND WHITE PHOTOGRAPHS
- ☐ GRAY SCALE DOCUMENTS
- ☐ LINES OR MARKS ON ORIGINAL DOCUMENT
- ☐ REFERENCE(S) OR EXHIBIT(S) SUBMITTED ARE POOR QUALITY
- ☐ OTHER: \_\_\_\_\_

**IMAGES ARE BEST AVAILABLE COPY.**

**As rescanning these documents will not correct the image problems checked, please do not report these problems to the IFW Image Problem Mailbox.**